

Anisotropy of subjective brightness
revealed by pupillary response
(瞳孔反応からみた主観的な明るさの異方性)

September 2022

Doctor of Philosophy (Engineering)

Novera Istiqomah
ノベラ イスティコマ

Toyohashi University of Technology

別紙 4 – 1 (課程博士 (英文))

Date of Submission (month, day, year) : September 21st, 2022

Department of Computer Science and Engineering	Student ID Number	D199303	Supervisors	Shigeki Nakauchi Tetsuto Minami
Applicant's name	Novera Istiqomah			

Abstract (Doctor)

Title of Thesis	Anisotropy of subjective brightness revealed by pupillary response
-----------------	--

Approx. 800 words

Anisotropy in the visual field (VF) has been investigated in terms of spatial resolution of attention, spatial frequency, and semantic processing. Brightness perception differences are also reported between the VFs. The brightness perception is evoked by the mismatch between the physical luminance and the subjective perceptual of the stimuli. Brightness perception can be influenced by low- (objects' surface reflectance) and high-order cognition (human memory system). Furthermore, indexing the subjective brightness perception by measuring pupil diameter (pupillometry) has been successfully demonstrated and showed its correlation to cognitive factors (e.g., memory and visual experience). For example, to test the effect of high-order cognition on subjective brightness perception using pupillometry, colored glare illusion was presented in the previous study, and it is proven that the ecological factors influenced subjective brightness perception. The glare illusion is a robust optical illusion to enhance the perceived brightness of a central white area surrounded by a luminance gradient. Many studies to understand cognitive load (low- and high-order cognition) influence on subjective brightness perception instructed the participants to fixate their gaze on a reference object and keep their heads stable, and used the presented stimuli's content. However, the anisotropy of subjective brightness perception in the peripheral VFs and world-centered coordinates by performing pupillometry and presenting the glare illusion remains have not been investigated.

Motivated by these challenges, this thesis aims to investigate the anisotropy of subjective brightness perception in the peripheral VFs and world-centered coordinates by manipulating the retinal and world-centered coordinates using pupillometry that reflects subjective brightness perception.

Before doing the main studies in this thesis, a preliminary study was conducted to contribute to additional evidence that perception is more predominant than the physical luminance of image stimuli by investigating the pupillary response to the ambiguous images of the sun and moon and instructing the participants to fixate their eyes and keep their heads stable during the stimuli presentation. The result of the preliminary study showed constricted pupils in response to the image perceived as the sun image despite the fact that the average physical luminance of sun images was lower than moon images. Thereafter, two primary experiments in this thesis were conducted.

First, by manipulating the retinal coordinates, the pupillary response to the glare illusion and halo stimuli in peripheral (upper, lower, left, and right) VFs were measured. The upper visual field (UVF) generated the highest degree of stimulus-evoked pupil dilation due to the disadvantages of UVF (spatial resolution of attention, visual accuracy, and contrast sensitivity – low-order cognition), and the highest degree of reduced pupil dilation in response to the glare illusion compare with other VFs might be influenced by the cognitive bias formed by statistical regularity in the processing of natural scenes in the UVF (higher-order cognition). These results confirm that low- and higher-order cognition evoked VFs anisotropy on subjective brightness perception.

Second, to investigate the anisotropy of subjective brightness perception in the world-centered coordinates, a further experiment was conducted by manipulating the world-centered coordinates, the pupillary responses to the glare and halo stimuli in a virtual reality (VR) environment (top, bottom, left, right, and center positions) were measured with (*active scene* experiment) and without head movement (*passive scene* experiment). The bottom location obtained the highest degree of pupil constriction caused by the bottom location linked to the peripersonal region by Previc (1998). In addition, the stimuli at the top location were perceived as darker than the bottom, which may be formed by statistical regularity in the processing of natural scenes (e.g., the influence of the bright sky). These results indicate that the extraretinal information influenced subjective brightness perception in the world-centered coordinates and

demonstrate the independence of pupillary response from head movement.

This thesis is part of a growing body on the anisotropy of subjective brightness perception in VFs and world-centered coordinates may be affected by the high-order cognition derived from the cognitive bias formed by statistical regularity in the processing of natural scenes (e.g., the sun's existence) in using glare illusion and pupillometry method. Besides, the results of this thesis would be contributions to informing architectural, light, and application design of a glare source (such as improving nighttime driving behavior) and to the ophthalmology field owing to the findings of the independence of head movement in pupillary response to the stimuli.

Acknowledgment

I greatly thank my supervisor Prof. Shigeki Nakauchi for his support, guidance, and advice from the very beginning, Prof. Tetsuto Minami for his support, guidance, and his advice as well, Dr. Kyoko Hine for her mentorship and support, Ms. Yuki Kawai for supporting my student's life, Dr. Yuta Suzuki, Yuya Kinzuka, Dr. Fumiaki Sato for their support and meaningful discussion, lab members in the doctoral room for our meaningful discussion and good times together, all visual perception and cognition (VPAC) lab members for meaningful discussion, international students in this university for their support on my research and good times together. I also greatly thank my husband, Qidun Maulana Binu Soesanto, my son for unconditional love, support and everything, my mother (in law), father (in law), and my family as my support system in Indonesia and everywhere they are for their support. I gratefully acknowledge the financial support from Amano Corporation Japan who awarded me with Amano Scholarship.

Table of Contents

Acknowledgment	iv
Table of Contents.....	v
List of Figures	viii
List of Tables.....	ix
Chapter 1:	
Introduction	1
1.1 Visual field anisotropy	1
1.2 Brightness perception.....	1
1.3 Pupillometry	2
1.4 Glare illusion	3
1.5 The human visual system	3
1.5.1 Visual area 1 (V1) – The primary visual cortex.....	6
1.5.2 Visual area 2 (V2) – The prestriate cortex	6
1.5.3 Dorsal and ventral stream.....	6
1.5.4 Extrastriate areas	6
1.6 Research questions and objectives	7
1.7 Structure of thesis.....	8
Chapter 2:	
Paper 1: The effect of ambiguous image on pupil response of sun and moon perception	11
2.1 Summary	11
2.2 Paper information.....	11
2.3 Abstract	12
2.4 Introduction	12
2.5 Methods.....	13
2.5.1 Observers.....	13
2.5.2 Stimuli and apparatus	13
2.5.3 Procedure.....	14
2.5.4 Pupil recording and analyses.....	15
2.5.5 Statistical analyses.....	15
2.6 Results and discussion.....	16
2.7 Conclusion.....	18

Chapter 3:**Paper 2: Anisotropy in the peripheral visual field based on pupil response to the glare**

	illusion	19
3.1	Summary.....	19
3.2	Paper information	19
3.3	Abstract.....	20
3.4	Introduction.....	20
3.5	Methods	22
3.5.1	Participants	22
3.5.2	Stimuli and apparatus	23
3.5.3	Procedure	24
3.5.4	Pupil recording and analyses	25
3.5.5	Statistical analyses	26
3.6	Results.....	27
3.7	Discussion.....	32
3.8	Conclusion	34

Chapter 4:**Paper 3: Brightness perception in world-centered coordinates assessed by pupillometry**

	36
4.1	Summary.....	36
4.2	Paper information	36
4.3	Abstract.....	37
4.4	Introduction.....	37
4.5	Materials & Methods	41
4.5.1	Participants	41
4.5.2	Stimuli and apparatus	41
4.5.3	Procedure	42
4.5.4	Pupil and eye gaze analyses.....	44
4.5.5	Statistical analyses	46
4.6	Results.....	46
4.7	Discussion.....	51
4.8	Conclusions.....	54

Chapter 5:

	General Discussion	55
--	---------------------------------	-----------

5.1	Overview of previous chapters.....	55
5.2	Challenges and limitations	57
5.3	Further work.....	59
Chapter 6:		
Conclusion		60
6.1	Findings.....	60
6.2	Contributions	61
References		62

List of Figures

Figure 1. 1. Simultaneous brightness contrast [1].....	2
Figure 1. 2. Pupil constriction and dilation.	2
Figure 1. 3. Human visual pathways	4
Figure 1. 4. Human visual cortex	5
Figure 1. 1. Simultaneous brightness contrast	2
Figure 1. 2. Pupil constriction and dilation	2
Figure 1. 3. Human visual pathways.....	4
Figure 1. 4. Human visual cortex.....	5
Figure 2. 1. Example of (a) sun and (b) moon images as a stimulus	14
Figure 2. 2. Experimental stimuli design.	15
Figure 2. 3. Pupillary change in response to the stimuli.....	17
Figure 3. 1. Experimental stimuli	24
Figure 3. 2. Experimental setup and procedure	25
Figure 3. 3. An initial local maximum negative value of the slope pupillary response	27
Figure 3. 4. Pupillary changes in five locations (center, upper, lower, left, and right)	28
Figure 3. 5. Early and late components of pupillary changes	30
Figure 4. 1. Experimental stimuli	42
Figure 4. 2. Experimental procedure	44
Figure 4. 3. Pupil size changes in the five locations (top, bottom, left, right, and center) in the world-centered coordinates.....	45
Figure 4. 4. Pupillary response to the glare and halo stimuli in the early component.....	47
Figure 4. 5. Descriptive plots of Bayesian rmANOVA in the late component	50
Figure 5. 1. Schematic of the main studies' results	56

List of Tables

Table 2. 1. Paired sample t-test of pupillary response for 3 s during the presentation phase ..	16
Table 2. 2. Paired sample t-test of pupillary response from PLR (1 s) during the presentation phase	16
Table 2. 3. Responses ratio to image type and percentage (%) of correct responses.....	17
Table 2. 4. Paired sample t-test of X and Y axis gaze data during the presentation phase	17
Table 3. 1. Main effects of analysis of variance in the early component	29
Table 3. 2. Multiple comparisons for visual field locations in the early component.....	29
Table 3. 3. Multiple comparisons for the interaction in the early component.....	31
Table 3. 4. Main effects of analysis of variance in the late component.....	31
Table 3. 5. Multiple comparisons for visual field locations in the late component.....	32
Table 3. 6. Multiple comparisons for the interaction in the late component	32
Table 4. 1. The main effect of three-way rmANOVA in the early component	47
Table 4. 2. Model comparison using Bayesian rmANOVA in the early component	48
Table 4. 3. The main effect of a three-way rmANOVA in the late component.....	49
Table 4. 4. Model comparison using Bayesian rmANOVA in the late component.....	49
Table 4. 5. The main effect of three-way repeated measures ANOVA in y-axis gaze data	50
Table 4. 6. Model comparison using Bayesian rmANOVA in y-axis gaze data	50

Chapter 1

Introduction

1.1 Visual field anisotropy

Visual field (VF) refers to an area in which the objects are visible to the observer during gaze fixation in one direction. There are two sorts of human VFs, i.e., the monocular and binocular VFs. The monocular VF is the visual field of only one eye, either the left or right eye. On the other hand, the binocular VF is the overlap area of monocular VFs. Binocular VFs divided by vertical and horizontal meridian is referred to as upper, lower, left, and right VFs. Besides, the central VF (the macula vision) is used in a task requiring central vision.

In recent years, research into the occurrence of different visual perceptions in VFs has gained [1]–[4]. Particularly, bias toward the upper VF (UVF) & right VF in the vertical and horizontal meridians, respectively, have been confirmed as the dominant effect in human VF by conducting matching-type tasks (name identity match and physical identity match) and varying their probability [5]. Following this, Previc et al. (2005) revealed the existence of mechanisms bias toward upper VF (UVF) in visual search tasks and semantic processing derived from the complex top-down processing due to the high-order cognition linked to the memory system to achieve optimal performance in the human visual system [6]. The UVF provides a higher pupil sensitivity to light changes during psychophysical experiments needing attentional resources [7]–[11]. In addition, previous studies reported the superior of UVF in motor-related tasks, visual search tasks, and semantic understanding [5], [6], [12]. In the context of bioecology factors, the human 3D spatial interaction proposed by Previc (1998) mentioned that the extrapersonal area has a scene memory advantage and is linked to UVF bias with 2 m and higher extension from the gaze-centered [12]. Consequently, the objects placed in the UVF are perceived as being farther in space. On the other hand, the peripheral area has a visual grasping function and bias toward lower VF (LVF) within a 1 m extension from the body. Thus, the objects placed in the LVF are perceived as nearer space. Besides, the superior of LVF is proceed the spatial frequency and spatial resolution sensitivity [13].

1.2 Brightness perception

The mismatch between the subjective light intensity perception and the actual physical light entering the retina (brightness perception) is one of the fundamental aspects of human visual processing. The brightness perception is influenced by the surface reflectance, regardless

of the object surface's illumination level (brightness constancy). For example, white paper (absorbed light intensity lesser than black paper) indoors is physically less intense than black paper outdoors, yet the white paper is seen as white and the black paper as black (perceptual constancy) due to the mechanisms of the light/dark adaptation in the retina. Furthermore, the background color of the objects evokes different brightness perceptions, known as simultaneous brightness contrast. For instance, the gray squares (physically identical luminance) surrounded by white backgrounds are perceived as brighter and surrounded by black backgrounds as darker (can be seen in Figure 1.1). This phenomenon is explained by low-level visual processing through the photoreceptors [14]–[16].

In addition, the human memory system affects the objects' perceived brightness. For example, the image and painting of the sun evoked a brighter perception than the image and painting of the moon despite having identical mean luminance [17], [18]. These samples are not coming from retinal processing yet a series of visual processing in the human brain, which requires the brain interpretation relating to the external world. In the example cases mentioned before, the perceived brightness was influenced by the cognitive load triggered by the ecological factor relating to the sun's existence, which included in the high level of human visual processing [17]–[19].

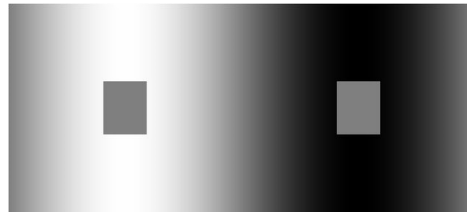


Figure 1. 1. Simultaneous brightness contrast [1]

1.3 Pupillometry

One of the five senses in humans is the eyes. Much information from the external world can be obtained from the eyes. The eyes can control the amount of light entering the retina through an iris by adjusting pupil size. The pupil response primarily depends on the light intensity. The pupil dilates in a dim environment to increase retinal luminance controlled by dilator muscles; contrary to this, the pupil controlled by the sphincter muscles constricts to decrease retinal illumination in a bright environment [20]–[22]. Figure 1.2

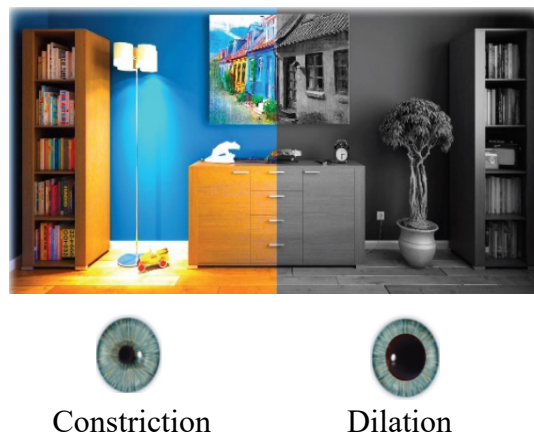


Figure 1. 2. Pupil constriction and dilation.

shows pupil performance in a bright (constriction) and dim (dilation) environment. Measuring pupil size in response to stimuli is known as pupillometry.

Furthermore, the pupillary response is initially represented as the pupillary light reflex (PLR) and followed by a reflection of various cognitive states. Besides, pupil diameter is influenced by visual attention, processed, and the subjective interpretation of light brightness. For example, Laeng and Sulutvedt (2014) revealed larger pupil constriction in response to the imagining of "looking at a sunny sky" and the "face of their mother" under the sunlight [23]. The other relevant study by Mathôt et al. (2017) conducted an experiment by presenting single words. They revealed that the words delivering a brightness sense generated more constricted pupils than those delivering a darkness sense [24]. The pupil size changes reflected the pupillary responses to the light source that has the potential to damage the eyes despite only occurring in observers' imaginations. Following this, Suzuki et al. (2019) conducted an experiment to investigate the influence of different illusion colors on brightness perception using the pupillometry method [25]. A larger pupillary constriction was yielded in response to the blue glare illusion due to the ecological factors relating to a dominant color in natural scenes (the blue sky). Recently, a previous study found that a larger pupil diameter reflects participants' judgment of the lightness as darker and vice versa [26]. It indicated the influence of pupillometry on subjective brightness perception. Thus, the pupillometry method can be used as an index of subjective brightness perception involving high-order cognition.

1.4 Glare illusion

An optical illusion is an illusion induced by the visual system and the visual perception that appears different from the physical luminance. For example, the previous study by Laeng and Endestad (2012) showed that optical illusion (glare illusion) appeared brighter than the physical luminance generated larger constricted pupils [27]. The glare illusion has been used in previous studies, confirming the robustness of brightness enhancement by the converging luminance gradient toward the pattern's center [25], [28], [29].

1.5 The human visual system

After the light rays hit the retina, the photoreceptor consisting of the rods (when the light source is very dim, scotopic vision) and cones (when there is plenty of light, photopic vision) will distribute input signal throughout the retina geniculate striate pathways that begin with the axon from the retinal ganglion cells in each eye forming the optic nerve and pass through the

lateral geniculate nucleus in the thalamus. Subsequently, the input signals from the left visual field (VF) are carried to the right primary visual cortex (visual area 1, V1) and vice versa (Figure 1.3). The visual cortex subdivision in humans is shown in Figure 1.4. (A).

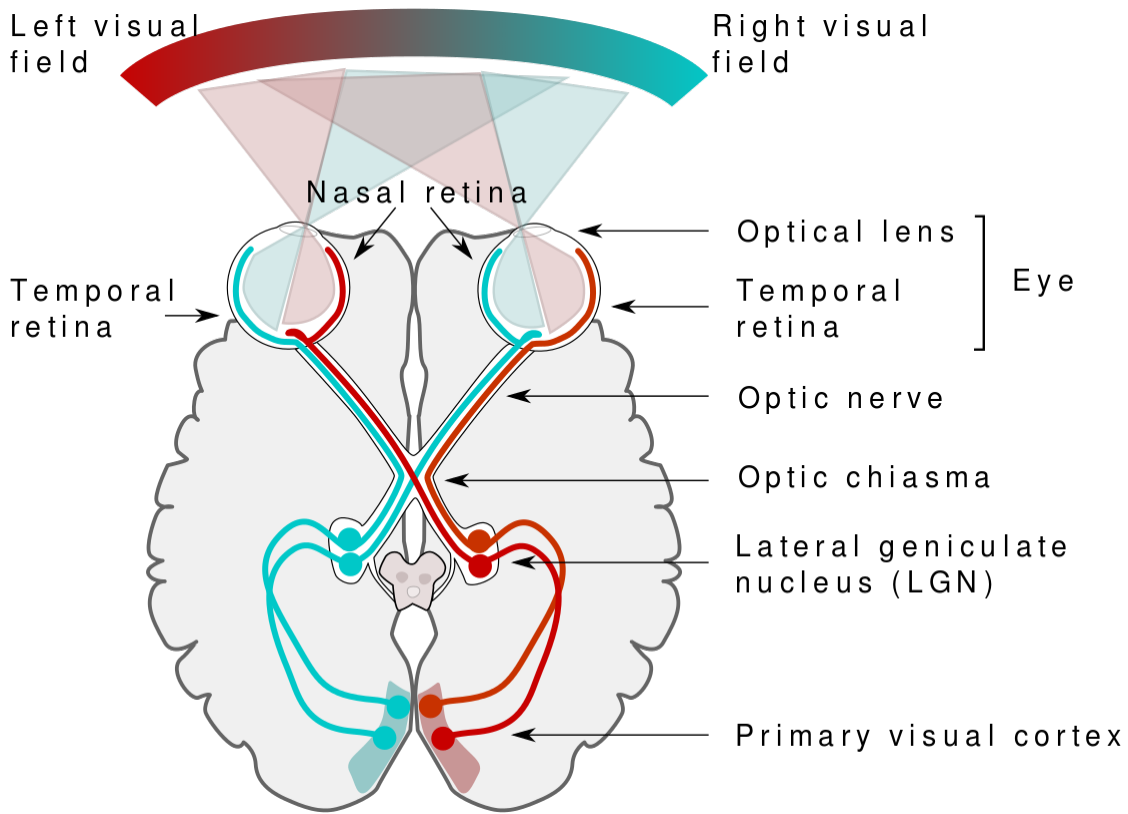


Figure 1. 3. Human visual pathways [30]

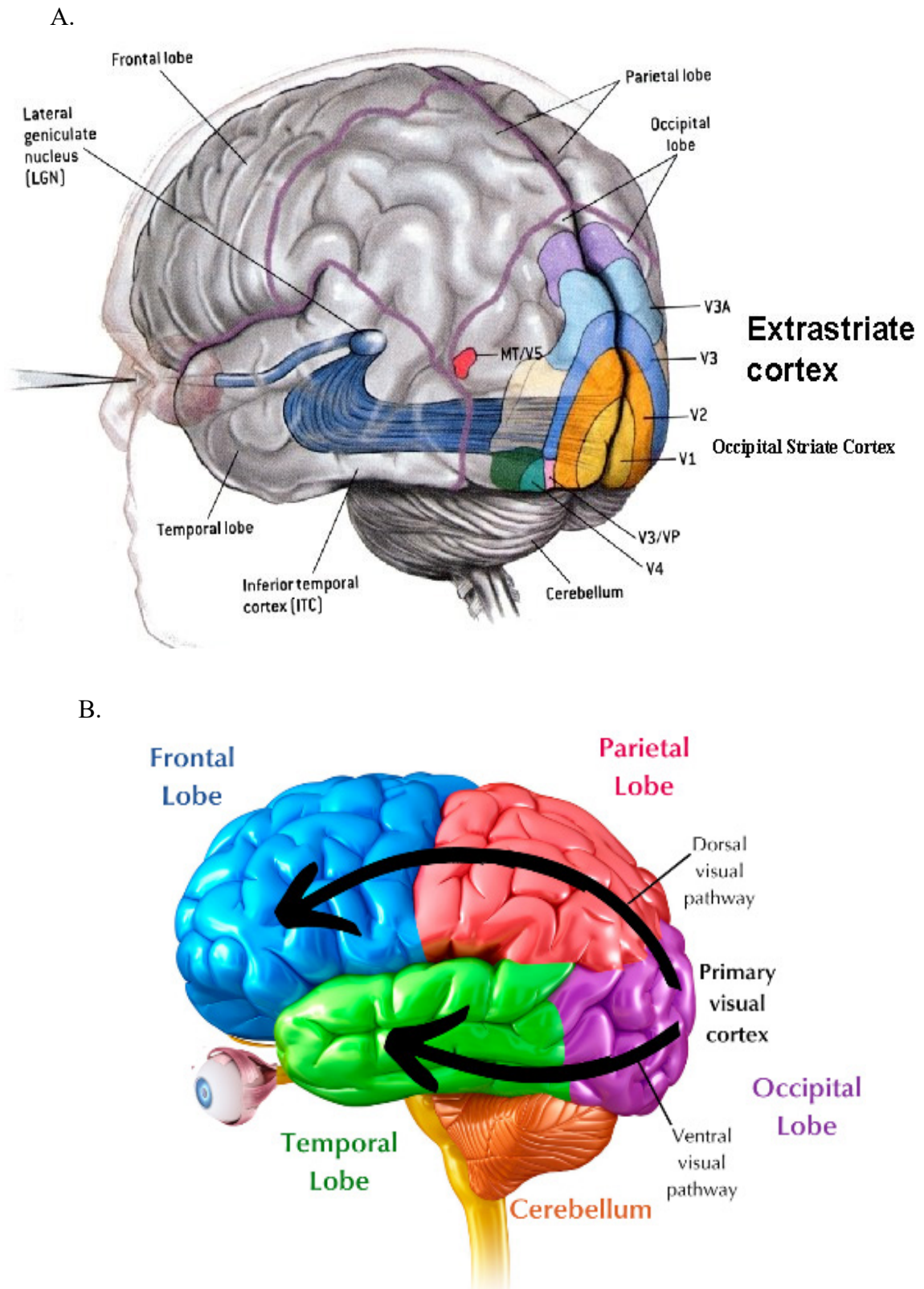


Figure 1. 4. Human visual cortex. (A) Visual cortex subdivision in human [31], (B) dorsal and ventral stream in human visual processing [32].

1.5.1 Visual area 1 (V1) – The primary visual cortex

The primary visual cortex (V1) contains receptive fields and has the task of extracting the fundamental visual features. Thus, the V1 is the best-understood area in the human visual system. The neighbouring parts of the visual scene's input on the retina are projected in the V1 without preserving the distance properties. However, the V1 will maintain the geometric relation of the local adjacent parts, widely known as a retinotopic map [6]. Retinotopic mapping, apart from that in V1 and V2, is complex, especially that in V4 [13].

1.5.2 Visual area 2 (V2) – The prestriate cortex

V2 is strongly connected to V1 (feedforward and feedback connection), visual area 3 (V3), visual area 4 (V4), and visual area 5 (V5). Despite having less well understanding than V1, V2 has similar tasks to V1 by combining the features of V1 tuned to orientation, spatial frequency, and more complex patterns [14]. Input signal from the V1 projected to the V2 via ventral stream reflecting the natural world's interpretation.

1.5.3 Dorsal and ventral stream

The human visual cortex relies on two processing streams, i.e., dorsal and ventral. The dorsal stream (the "where" stream) originates in the V1 to V2 in the occipital lobe passing dorsally through the parietal lobe and is associated with motion. On the other hand, the ventral stream (the "what" stream) distributes the input signal ventrally from the V1 to V2 into the inferior temporal cortex through V4 and is related to shape perception and object recognition. Detailed figures of dorsal and ventral streams can be found in Figure 1.4B.

1.5.4 Extrastriate areas

Extrastriate areas are referred to as beyond the V1 of the visual cortex area. Computing more complex and abstract features are the role of extrastriate areas. These areas have not well understood the input signal, yet informative for the brain to interpret the input signal. Extrastriate areas consist of V3, V4, V5, and the inferior temporal (IT) cortex.

V3 is linked to V2 responding to global motions. V4 lies on the ventral visual pathway and proceeds the high complexity shapes as well as the quantity of color sensitivity. V5 responds the complex motion patterns. In addition, ITC processes the merged information of both halves' VFs and the recognition of complex shapes by parsing them into simpler shapes.

1.6 Research questions and objectives

Previous studies have presented that subjective perceptual brightness modulation represented by the pupil diameter is associated with cognitive factors, such as memory and visual experience using the images and painting of the sun and moon [17], [18]. In addition, previous work adopted the colored glare illusion and pupillometry method [25]. It confirmed that the blue glare illusion was subjectively evaluated as the brightest condition in a psychophysical adjustment task might be due to the cognitive bias relating to the natural scene where "the sun shining in the blue sky". However, the anisotropy of subjective brightness perception in peripheral VFs and world-centered coordinates using glare illusion and pupillometry methods remains unclear. Therefore, this thesis aims to investigate the anisotropy of subjective brightness perception in peripheral VFs (upper, lower, left, and right) and world-centered coordinates (top, bottom, left, right, and center positions) based on pupillary response to the stimuli (glare and halo) through two main experiments (Experiment 1 and Experiment 2). The findings of this thesis provide new valuable insights into the anisotropy of subjective brightness perception in VFs and world-centered coordinates revealed by pupillary response to the glare illusion, as well as in the ophthalmology field that the pupillary response is not affected by head movement.

Yet, before conducting two main experiments in this thesis project, a preliminary study was performed. This preliminary study (*Paper 1 - The Effect of Ambiguous Image on Pupil Response of Sun and Moon Perception*) investigate the pupillary response to ambiguous images of the sun and moon to gain an understanding of the subjective brightness perception in response to the image stimulus perceived as the sun or moon while the participants fixated their gaze on a reference object in the middle of stimuli image during the stimuli presentation. This preliminary study was conducted to provide additional evidence that the perception of the image stimuli as the sun or moon image takes a more important role than the physical luminance, and it might be influenced by ecological factors such as the sun's existence. This perception which exhibits the influence of the sun's existence (from the top) on the subjective brightness perception, will have an important account in Experiment 2's findings in this thesis project.

The objectives of this thesis are as below:

1. *Experiment 1 (Paper 2 - Anisotropy in the peripheral visual field based on pupil response to the glare illusion)* investigate the pupillary response to the glare and halo stimuli by manipulating the retinal coordinates (placing the stimuli in peripheral VFs, i.e., upper,

lower, left, and right) to identify the anisotropy of subjective brightness perception in peripheral VFs, particularly the influence of the ecological factors relating to the statistical regularity in natural scenes indexed by the pupil diameter change while the participants' gaze was fixed to a fixation cross in the middle of stimuli for 4 seconds.

2. *Experiment 2 (Paper 3 - Brightness perception in world-centered coordinates assessed by pupillometry)*
 - a. Conduct active and passive scene experiments to rule out the low- from high-order cognition by presenting glare and halo stimuli in five positions in the world-centered coordinates and measuring the pupil size changes.
 - b. Split the pupillary responses based on the peak of PLR magnitude into early and late components to distinguish data between PLR and the pupil recovery after the PLR until the stimulus offset using programming software.
 - c. Compare and analyze the pupillary response to the stimuli between early and late components in the active and passive scene experiments to investigate the influence of high-order cognition on the subjective brightness perception indexed by the pupillary responses in the five positions in the world-centered coordinates.
 - d. Compare and analyze the y-axis of gaze data between early and late components in the active and passive scene experiments to verify that the retinal coordinates were identical, which can be evidence of the relationship between head movement and pupillary responses.

1.7 Structure of thesis

To structure this thesis, two main topics have been elucidated and conducted in two main experiments. Experiment 1 defines anisotropy of subjective brightness perception in peripheral VF by manipulating retinal coordinates, and experiment 2 in the world-centered coordinates by manipulating world-centered coordinates. Besides, the preliminary study was added before conducting two main experiments. In this thesis, two approaches have been developed and validated based on pupillary response to the glare illusion. This thesis consists of six chapters. Note that the preliminary study and main topics, and their respective publications are highly linked among each other. Some parts of the following text within this chapter are excerpts of the various publications presented within this dissertation.

Chapter 1: Introduction. The introduction section shows this thesis's relevant background information, research questions, objectives, and overview.

Chapter 2: Paper 1: The Effect of Ambiguous Image on Pupil Response of Sun and Moon Perception. This chapter represents the preliminary study of this thesis project conducted before two main experiments.

Background: The previous studies, pupil size change is known to be influenced by the stimulus form that depends on the lightness on its surface appearance, light source, or illusion forms [27], [33], [34]. Recently, Binda et al., and Castellotti et al., reported that the constricted pupil in response to sun images and paintings is influenced by high-level cognition and not only by the physical light intensity [17], [18]. The pupil change in response to the sun's image and painting on the individual brightness levels is believed as an independent response from the perceived actual light. However, previous studies have not been able to segregate the physical factors from the cognitive factors associated with image stimulus.

Outcome: By segregating the physical factors from the cognitive factors associated with the image stimulus, additional evidence has been contributed that subjective brightness perception has an essential role over physical luminance. The experiment in the preliminary study has been conducted and successfully analyzed within this doctoral project. In detail, the explanation of the preliminary study is presented in **Paper 1**.

Chapter 3: Paper 2: Anisotropy in the peripheral visual field based on pupil response to the glare illusion. Chapter 3 explains experiment 1, which defines anisotropy of subjective brightness perception in peripheral VF by manipulating retinal coordinates.

Background: Previous works using a glare illusion with “blue” converging gradients, which was subjectively evaluated as the brightest condition in a psychophysical adjustment task and elicited the most significant changes in large pupil constriction compared with other colors, were conducted [35]. Part of the brightness enhancement may be attributed to the cognitive bias formed by statistical regularity in natural scene processing: the cognitive bias created by the visual property difference that ensues in natural scenes where “the sun shining in the blue sky” may be associated with the blue glare illusion and induce prominent pupil constriction. The extent to which brightness perception is induced by VF anisotropy remains unclear. Specifically, it is unclear how the predominant understanding of ecologically explained cognitive bias, formed by statistical regularity in natural scenes in the VF (e.g., the light-from-above bias), affects brightness perception.

Outcome: By manipulating the retinal coordinates and investigating the pupillary response to the stimuli located in peripheral VF, a new valuable insight into VF anisotropy of subjective brightness perception in peripheral VF benefits many applications, such as in informing the design of applications aimed at improving nighttime driving behavior. The approach has been implemented and successfully validated in **Paper 2**.

Chapter 4: Paper 3: Brightness perception in world-centered coordinates assessed by pupillometry. This chapter shows the methods of experiment 2 that investigate the anisotropy of subjective brightness perception in the world-centered coordinates by maintaining the identical retinal coordinates.

Background: After conducting experiment 1, an issue arose. In experiment 1, the anisotropy of subjective brightness perception in the peripheral VF was influenced by low- and higher-order cognition by manipulating the retinal coordinates. However, Experiment 1's results raise the possibility that the differences in retinal coordinates and many opponent processes in the human visual system will affect the subjective brightness perception in the VFs.

Outcome: To investigate the anisotropy of subjective brightness perception in the world-centered coordinates, we presented the glare and halo as the stimuli in five different positions (top, bottom, left, right, and center) in the world-centered coordinates and measured the pupil diameter in response to the stimuli during the stimulus presentation while the observers fixated on the fixation cross located in the middle of stimulus. By manipulating the world-centered coordinates, experiment 2 successfully investigate the anisotropy of subjective brightness perception in the world-centered coordinates and has been presented thoroughly in **Paper 3**.

Chapter 5: General discussions. This chapter contains a general discussion of the preliminary study and the anisotropy of subjective brightness perception in peripheral VF (experiment 1) and in the world-centered coordinates (experiment 2).

Chapter 6: Conclusions. This chapter summarizes the findings and contributions of this thesis.

Chapter 2

Paper 1: The effect of ambiguous image on pupil response of sun and moon perception

2.1 Summary

Before conducting two main experiments in this thesis project, a preliminary study which explained the influence of ambiguous images of the sun and moon on subjective brightness perception was performed thoroughly in **Paper 1** within this chapter. Additional evidence regarding the importance of subjective brightness perception over the physical luminance of the stimuli is obtained from this preliminary study. The pupillary responses to the ambiguous images of the sun and moon were measured during the stimuli presentation for a few seconds. Thereafter, another few seconds required participants' feedback on whether they perceived a presented stimulus as the sun or moon. This preliminary study's results showed that pupillary response to the subjective brightness perception as sun images (perception, "PR") generated more constricted pupils than the pupillary response to the actual sun images (the ground truth, "GT"). In terms of ecological factors, the results were affected by high-level cognition related to the working memory of the sun's existence. The finding of this preliminary study will have an important account in Experiment 2's findings in this thesis.

2.2 Paper information

N. Istiqomah, T. Takeshita, Y. Kinzuka, T. Minami, and S. Nakauchi, "The Effect of Ambiguous Image on Pupil Response of Sun and Moon Perception," *International Symposium on Affective Science and Engineering*, vol. ISASE2022, pp. 1-4, 2022. <https://doi.org/10.5057/isase.2022-C000004>.

Reproduced from International Symposium on Affective Science and Engineering ISASE2022, 1-4 (2022), online on May 31st, 2022, published by Japan Society of Kansei Engineering, with minor modification.

Article 2 (Copyright) Copyrights and other rights regarding the Registered Data published on the Service belong to the Publishing Organizations or their authors, etc.

2.3 Abstract

This study investigates the influence of ambiguous sun and moon images on stimuli perception based on pupillometry. A random stimulus was presented in a few seconds, and another few seconds, as feedback, observers reported the stimulus was perceived as the moon or the sun. To overcome the lack of previous studies that have not been able to segregate the physical (Glare effect) and cognition factors of image stimulus, the data were grouped into two categories, i.e., as the actual image (the ground truth, “GT”) and observers’ perception (“PR”) responses. As a result, the pupil constricted significantly when the stimulus is perceived as the sun. Furthermore, this pupillary response is unassociated with the average physical luminance of images. This result indicates that high-level cognition influences perception pupillary response.

Keywords: *brightness perception, pupillometry, cognition, perception, glare effect*

2.4 Introduction

Much information can be obtained from the outside world that relies on the peripheral light in ambient surroundings through the eyes. The pupillary response primarily depends on the light intensity from this ambient surrounding. From the previous studies, pupil size change is known to be influenced by the stimulus form that depends on the lightness on its surface appearance, light source, or illusion forms [27], [33], [34], [36]. The illusion or stimulus brightness provided different perceptions between the source and perceived across the observers [37], known as the brightness perception. The assemblage of light’s physical intensity and various context-dependent variables affect the brightness perception in the human visual system. Hence, the brightness perception does not constantly match the physical light’s quantity from the source. This mismatch between individual brightness and physical luminance intensity is visible in greater constricted pupil phenomenon by bright illusion, a painting/cartoon depicting the sun, manipulated illusions similar to the sun or sun images [17], [27], [38].

Binda et al., Laeng et al., and Corney et al. reported that the constricted pupil in response to sun images is influenced by high-level cognition and not only by the physical light intensity [17], [27], [37]. The pupil change in response to the sun’s image on the individual brightness levels is believed as an independent response from the perceived actual light.

The pupil dilates in a dim environment to increase retinal illuminance; contrary, pupil constriction decreases retinal illumination to restrict the incident light in bright environments. These pupillary responses toward bright light (constricted pupil) are primarily carried out by activating the iris sphincter muscle and the iris dilator muscle's interaction, which mainly drives

pupillary dilation [39], [40]. Measuring the pupil size of these pupillary responses to the stimuli is called pupillometry, a physiological index reflecting multiple psychological states in humans.

The pupil size changes not only while observing a reflective object but also while looking at photographs and paintings, which convey the sense of brightness. However, previous studies have not been able to segregate the physical factors from the cognitive factors associated with the image stimulus. To further investigation, this study presented the ambiguous sun and moon images as the stimuli for a few seconds and in another few seconds to determine the stimulus as a moon or sun. Through the pupil change in response to the stimuli, as an index of subjective brightness perception, we provided the data into two methods, namely the actual image (the ground truth, hereinafter “GT”) and observers’ perception responses (hereinafter “PR”) of the sun images, and investigated whether the low-, high- or low- and high-level cognition influence the observers' perception of the sun and moon images. We hypothesized that low- and high-level cognition affect the PR conditions in response to the sun images. Thus, the current research’s finding is subjectively perceived brightness of the sun image induced by the high-level cognition, not only influenced by the physical luminance of the stimuli.

2.5 Methods

2.5.1 Observers

Twenty-one observers (21 males, average age of 23 years, standard deviation 1.3 years) participated in the experiment. All observers had a normal or corrected-to-normal vision and had filled consent form prior to their participation after procedural detail explanation. All experimental procedures were conducted according to the ethical principles outlined in the Declaration of Helsinki and approved by the Committee for Human Research at the Toyohashi University of Technology.

2.5.2 Stimuli and apparatus

The stimuli consist of 100 images in total, 50 images of the sun and moon. The original



Figure 2. 1. Example of (a) sun and (b) moon images as a stimulus

images were RGB images obtained by questing "sun" and "full moon" from *Pixabay*, a free stock photography website. We trimmed them to square images with the sun or moon at the center and converted them into grayscale images. To retain the context of the images, from all stimuli candidates, we excluded the images that have a partially hidden sun or moon and at size less than 400×400 pixels, also images containing people or text. The image stimulus was presented at 11.91 degrees on the display center. Furthermore, we averaged the luminance of the selected sun and moon images as the stimuli controlled by the SHINE toolbox of MATLAB [41]. The average luminance of the sun and moon images in the 2 degrees fovea are 74.87 and 76.95 cd/m^2 , respectively. Figure 2.1 shows an example of sun and moon images used in this experiment.

The experiment was conducted by MATLAB R2019b, Psychtoolbox-3.0.16 [9], and all stimuli were presented on a liquid-crystal display monitor (Display++, Cambridge Research Systems Ltd., Kent, UK) with a resolution of $1,920 \times 1,080$ pixels and a refresh rate of 120 Hz. The eye-tracking system (EyeLink 1000PLUS, SR Research, Oakland, Canada) was used to measure the pupil diameter and gaze movements at a sampling rate of 500 Hz during the experimental task. The tracking was based on "pupil diameter" using the centroid mode in the device setting.

2.5.3 Procedure

The experiment was conducted in a dark room, and all observers rested their chins at a fixed viewing distance of 70 cm from the monitor. The eye tracker was calibrated using a standard five-point calibration prior to the session. A fixation cross was presented on the monitor's center for 1 s in each trial. Afterward, a sun/moon image was randomly presented also on the monitor's center for 3 s. Then, observers were given a set of times to respond according to their perception of the stimulus (as sun/moon). Detailed experimental stimuli

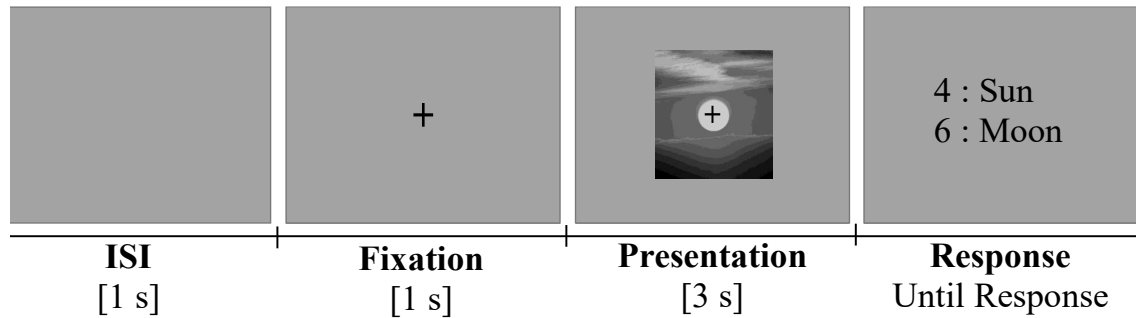


Figure 2. 2. Experimental stimuli design.

design can be seen in Figure 2.2. During the fixation cross and stimulus presentation, observers were instructed to refrain from blinking their eyes and were required to fixate on the central fixation cross. This experiment has 100 trials for each observer using 100 different images provided by the author.

2.5.4 Pupil recording and analyses

The eye-tracker generated pupil data in arbitrary units (a.u.) and recorded 2D gaze coordinated. The pupil data obtained as zero values during eye blinks were interpolated using cubic Hermite interpolation. Trials with additional artifacts (the velocity change in pupil size was more than 20 [a.u./s]) were excluded from the analysis. Additionally, a principal component analysis was performed at each time point for pupil size; when the Euclidian distance (calculated using the first and second principal components) was greater than $\pm 3\sigma$ of all trials, those were rejected. The average rejected trials were 14.6% of all trials per observer included in the following analysis. The baseline correction of pupillary response was performed by subtracting the average samples collected at 0.3 s before the stimulus onset. Finally, all data were converted to z-scores (z). This analysis was also applied to eye gaze data. Furthermore, the pupil data were epoched by the two conditions, GT and PR, during the presentation phase (3 s from onset).

2.5.5 Statistical analyses

The GT and PR methods were separately subjected to statistical analysis. We conducted paired sample t-tests to pairwise comparisons of the main effects between sun and moon images in each condition. Before applying this, we calculated the pupillary light reflex (PLR) average in each condition and observer and yielded 1 s of PLR for both conditions. The significance level (α) was set to $p < 0.05$ for all analyses. We also reported Bayesian Factor (BF), estimating

the relative weight of the evidence in favor of H_1 over H_0 as BF_{10} for t-tests [42]. All statistical analyses were performed using Jamovi 1.1.9.0 [10].

2.6 Results and discussion

Figure 2.3 represents the pupillary diameter change by the stimuli (sun/moon image) presented in the center of the monitor. We reported that the pupillary responses as PR data yielded a greater difference between sun and moon images' response than GT data. Figure 2.3A is used as a baseline to separate the data between PLR and the next area, and it shows that PLR occurred in the range between 0 s – 1 s.

Furthermore, we calculated the ratio between GT and PR conditions (see Table 2.3). The correct perception (sun images perceived as sun images and moon images perceived as moon images) has 68.27% in total, with 79.87% and 56.79% of correct sun and moon perception, respectively. The sun perception data is 61.44%, with 79.87% and 43.21% sun perception from sun and moon images, respectively.

Table 2. 1. Paired sample t-test of pupillary response for 3 s during the presentation phase

			Statistic	p	Δ Mean	Δ SE
GT	Sun vs. Moon	t	-1.95	0.065	0.0208	0.0107
		BF_{10}	1.11			
PR	Sun vs. Moon	t	-2.50	0.021*	0.0304	0.0122
		BF_{10}	2.69*			

Table 2. 2. Paired sample t-test of pupillary response from PLR (1 s) during the presentation phase

			Statistic	p	Δ Mean	Δ SE
GT	Sun vs. Moon	t	-1.95	0.066	0.0415	0.0213
		BF_{10}	1.11			
PR	Sun vs. Moon	t	-2.76	0.012*	0.0737	0.0267
		BF_{10}	4.32*			

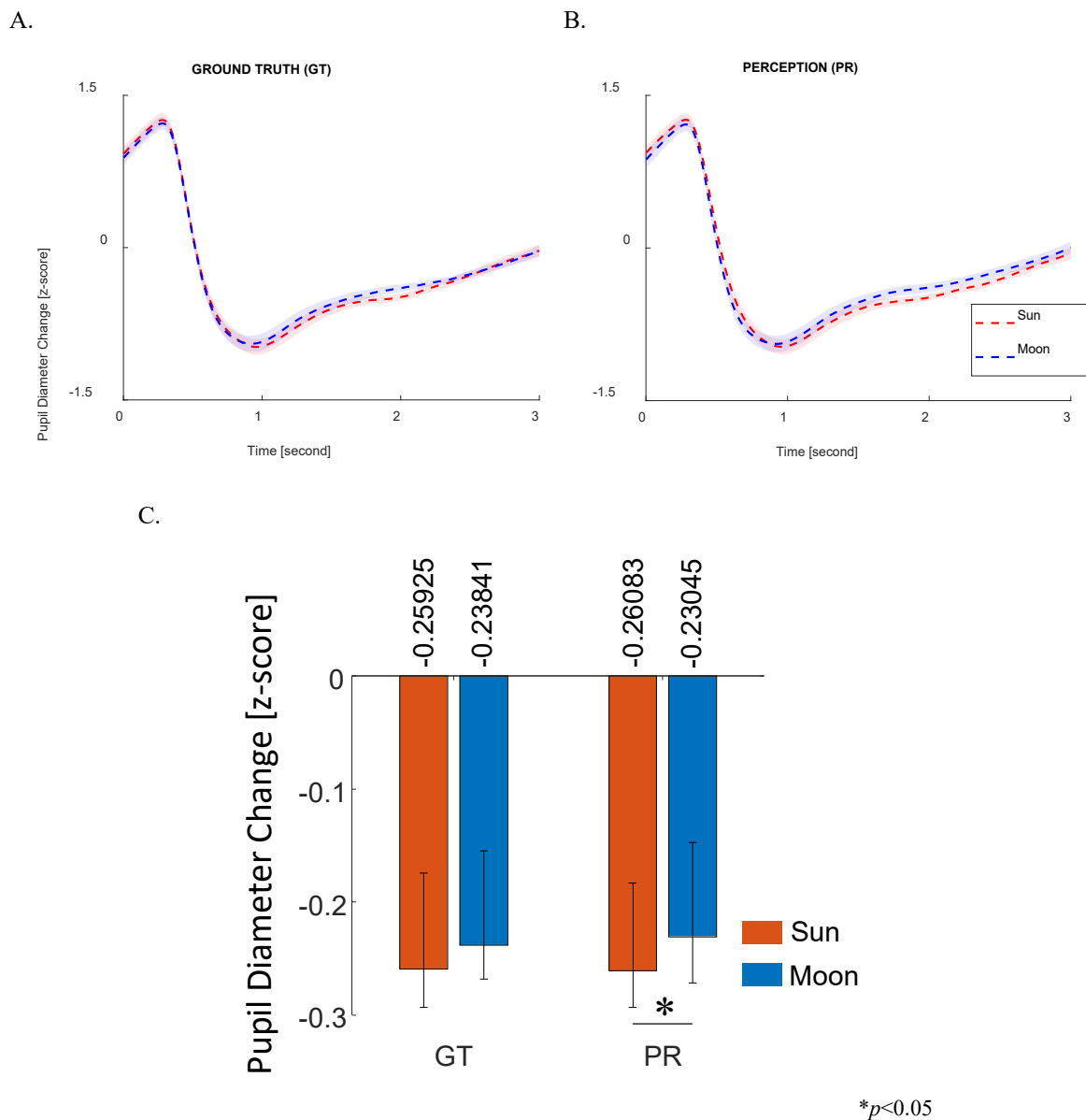


Figure 2. 3. Pupillary change in response to the stimuli. During stimuli onset in (A) GT and (B) PR categories, also (C) the average pupil diameter changes for 3 s in GT and PR.

Table 2. 3. Responses ratio to image type and percentage (%) of correct responses

	Perception (PR)			Correct
		Sun	Moon	
Ground Truth (GT)	Sun	79.87	20.13	79.87
	Moon	43.21	56.79	56.79
Total		61.44	38.56	68.27

Table 2. 4. Paired sample t-test of X and Y axis gaze data during the presentation phase

			Statistic	p	Δ Mean	Δ SE	
GT	X	Sun	t	0.560	0.581	0.0269	0.0480
		vs.	BF_{10}	0.262			
	Y	Moon	t	0.443	0.662	0.0198	0.0448

		BF ₁₀	0.249			
	X	t	1.334	0.197	0.0723	0.0542
		BF ₁₀	0.494			
PR	Y	t	2.586	0.018*	0.1407	0.0544
		BF ₁₀	3.152*			

This study conducted a pupil size measurement experiment to clarify whether cognitive factors influence the constricted pupil in response to the sun image perception. As a result, we confirmed a greater constricted pupil in response to the sun image in the PR condition compared with the pupil change of the GT condition. Furthermore, the presented image stimulus in the center of the monitor evoked the strongest constricted or dilated pupil [11].

The present study generated a greater constricted pupil only in the PR condition. Therefore, we hypothesized that cognitive factors induced pupil changes in response to the image stimulus perceived as the sun. Table 2.3 represents the percentage of the image stimulus perceived as the sun had a higher value than perceived as the moon. Moreover, the pupil changes on images stimulus perceived as the sun had larger constricted pupil even though the moon images' physical luminance was larger than sun images. It indicates that the constriction related to the sun perception is unrelated to the luminance difference in the fovea. As we expected, the result of the present study was influenced by high-level cognition.

2.7 Conclusion

In this study, the pupillometry method was used to investigate the influence of high-level cognition on pupil changes during the image stimulus presentation. The pupil diameter changes in response to the image stimulus perceived as the sun evoked a greater pupillary constriction than in GT condition even though the physical luminance average of the sun image was lower than the moon image. Moreover, the difference between the pupillary response to the sun and moon on the GT condition did not reach statistical significance. It strongly suggests that the actual luminance of the image stimulus is independent of the observers' perception. It may be induced by the experience in daily vision, preventing probable dazzling from the sun. Thus, the result in the present experiment was influenced by high-level cognition, particularly by preventing the hazardous light source (sunshine) from entering the eyes.

Chapter 3

Paper 2: Anisotropy in the peripheral visual field based on pupil response to the glare illusion

3.1 Summary

Within this paper, experiment 1 of this thesis project regarding anisotropy of subjective brightness perception in the peripheral VF was conducted. To achieve the first aim of this thesis, to identify the anisotropy of subjective brightness perception in peripheral VFs, first approach (by manipulating the retinal coordinates) is used and described in detail in **Paper 2** within this chapter.

Recently, multiple previous studies in VF anisotropy have been conducted associated with spatial frequency, spatial resolution of attention, and semantic processing. The brightness perception differences between VF also occurred. However, the VF anisotropy of subjective brightness perception in the peripheral VF remains unclear specifically based on the pupillary response to the glare illusion as an index of subjective brightness perception.

Within the first experiment, a random stimulus (glare or halo) was presented for a few seconds and the eye tracking measured the pupil size during the stimulus presentation. By separating the pupillary response into early and late components (area under curve, AUC) and analyzing those data, this experiment found greater stimulus-evoked pupillary dilation due to poor contrast sensitivity (low-order cognition) and glare-related dilated pupil reduction in the upper VF (UVF) compared with halo-related pupillary changes owing to the superior cognitive bias formed by statistical regularity in natural scene processing of the glare illusion in the UVF (higher-order cognition).

3.2 Paper information

N. Istiqomah, Y. Suzuki, Y. Kinzuka, T. Minami, and S. Nakauchi, “Anisotropy in the peripheral visual field based on pupil response to the glare illusion,” *Heliyon*, vol. 8, issue 6, pp. 1-7, 2022. <https://doi.org/10.1016/j.heliyon.2022.e09772>.

Reproduced from Heliyon, vol. 8, issue 6, pp. 1 – 7, June 24th, 2022 [e09772] published by Elsevier, with minor modification.

Journal Author Rights

Please note that, as the author of this Elsevier article, you retain the right to include it in a thesis or dissertation, provided it is not published commercially. Permission is not required, but please ensure that you reference the journal as the original source.

3.3 Abstract

Visual-field (VF) anisotropy has been investigated in terms of spatial resolution of attention, spatial frequency, and semantic processing. Brightness perception has also been reported to vary between VFs. However, the influence of VF anisotropy on brightness perception using pupillometry has not been investigated. The present study measured participants' pupil size during glare illusion, in which converging luminance gradients evoke brightness enhancement and a glowing impression on the central white area of the stimulus, and halo stimuli, in which the same physical brightness of the glare illusion is used with a diverging luminance pattern. The results revealed greater stimulus-evoked pupillary dilation and glare-related dilated pupil reduction in the upper VF (UVF) compared with other VFs and halo-related pupillary changes, respectively. The stimulus-evoked pupillary dilation was affected by poor contrast sensitivity. However, owing to the superior cognitive bias formed by statistical regularity in natural scene processing of the glare illusion in the UVF, we found reduced pupillary dilation compared with the response to halo stimuli and the response from other VFs. These findings offer valuable insight into a method to reduce the potential glare effect of any VF anisotropy induced by the glare effect experienced in daily vision. An important practical implication of our study may be in informing the design of applications aimed at improving nighttime driving behavior. We also believe that our study makes a significant contribution to the literature because it offers valuable insights into VF anisotropy using evidence from pupillometry and the glare illusion.

3.4 Introduction

The difference of observers' perception scale (slightly or significantly) in different visual fields (VFs) associated with the stimulus orientation is termed VF anisotropy. Multiple studies have demonstrated VF anisotropy in visual perception [12]–[15]. For example, the spatial resolution of attention and spatial frequency sensitivity is known to have an advantage in human vision, attributed to a downward bias in the lower VF (LVF) compared with the upper VF (UVF) [13]. In contrast, an advantage in the UVF is also reported in motor-related tasks, visual search tasks, and semantic understanding [1], [16], [17]. In the context of bioecology,

an object presented in the lower and upper hemifield is perceived as being placed closer and farther in space, respectively. This vertical VF segmentation may be enhanced by the function that enables individuals to experience a critical event more easily close-up for them to survive in the natural environment, whereas objects farther away need to be predicted accurately from a distance [43], [44]. These specific functions of vertical VFs have also been discussed from physiological perspectives. Specifically, previous studies that adapted pupillometry have suggested a higher pupil sensitivity to light changes in the UVF during an attention task [7]–[11], [45], [46].

Apparent brightness perception is reported to vary between VFs [47]. Brightness perception in the visual system is determined by a confluence of the physical intensity of light and several context-dependent factors. Thus, brightness perception does not always match the quantity of physical light from the source. McCourt et al. (2013) conducted an illumination intensity matching task and reported that an illuminated object from the LVF is perceived as more illuminated compared with an illuminated object from the UVF owing to light adaptation that takes more time [48]. This mismatch between subjective brightness and physical luminance intensity has also been seen in the phenomenon of a larger pupillary constriction evoked by a bright illusion [27], the sun's image [48], or a painting depicting the sun [17] that appears perceptually brighter.

Pupillometry, the measurement of pupil size, is a physiological index that reflects multiple cognitive states across species. Parts of the autonomic nervous system and the parasympathetic and sympathetic nervous systems regulate the iris sphincter and dilator muscles, respectively [28], [49]–[53]. Apart from functioning as a reflex to light, the pupil also reacts to subjective brightness perception. Laeng and Endestad (2012) initially reported that an optical illusion in which an object appears brighter than its physical luminance evokes larger pupil constriction [27]. This optical illusion is called the “glare illusion” and provokes robust brightness enhancement by a luminance gradient that converges toward the center of the pattern [25], [54]. Zavagno et al. found that the illusory perception emerged from the luminance gradient that caused not fully segregate the background and target area conducting the rating task experiment between the areas using luminance contours, illusory contours, no contours, and ambiguous contours [55]. The results were highly influenced by the process of segregation between the target area and the background combined with the luminance gradient attendance. Furthermore, previous research also used a glare illusion with “blue” converging gradients, which was subjectively evaluated as the brightest condition in a psychophysical adjustment task and elicited the most significant changes in large pupil constriction compared with other

colors [25]. Part of the brightness enhancement may be attributed to the cognitive bias formed by statistical regularity in natural scene processing: the cognitive bias created by the visual property difference that ensues in natural scenes where “the sun shining in the blue sky” may be associated with the blue glare illusion and induce prominent pupil constriction [25]. The extent to which brightness perception is induced by VF anisotropy remains unclear. Specifically, it is unclear how the predominant understanding of ecologically explained cognitive bias, formed by statistical regularity in natural scenes in the VF (e.g., the light-from-above bias), affects brightness perception. Therefore, this study aimed to elucidate if visual processing conveying a dazzling effect in the glare illusion also has an ecological advantage in the VF.

We compared pupil size changes as stimuli (glare illusion and halo stimuli) were presented for a few seconds in five VF locations (upper, lower, left, right, and center). The changes in pupil size were regarded as an index of subjective brightness perception. From both ecological and anatomical points of view, pupillary response to the glare illusion was expected to vary across different VFs. We hypothesized that the differences in pupil changes between the glare illusion and halo stimuli in the UVF would be larger than those in the other positions owing to ecological factors, such as the representation of the sun and assumptions that the light source is in the UVF [54], [56]. Additionally, constricted pupils may occur in response to stimuli in the LVF owing to the advantage of spatial resolution and visual accuracy in the LVF [9], [57]. Thus, this research integrated pupillometry as an index of subjectively perceived brightness in anisotropic fields, especially focusing on the effect of the vertical hemifield.

3.5 Methods

3.5.1 Participants

Twenty-two undergraduate and graduate students (9 men and 13 women), aged between 23 and 33 years (mean 26.86, SD 3.90 years), participated in the experiment. All participants had a normal or corrected-to-normal vision. Two participants were excluded from the analysis for recording 50% more eye blinks in all trials or invalid trials, the data of which could not be interpolated at the pre-processing stage. All experimental procedures were conducted according to the ethical principles outlined in the Declaration of Helsinki and approved by the Committee for Human Research at the Toyohashi University of Technology. The experiment was conducted with complete adherence to the approved guidelines of the committee. Informed written consent was obtained from the participants after procedural details had been explained

to them. The raw data and analysis codes are available at <https://github.com/suzuki970/GlarePupilAnisotropy>.

3.5.2 Stimuli and apparatus

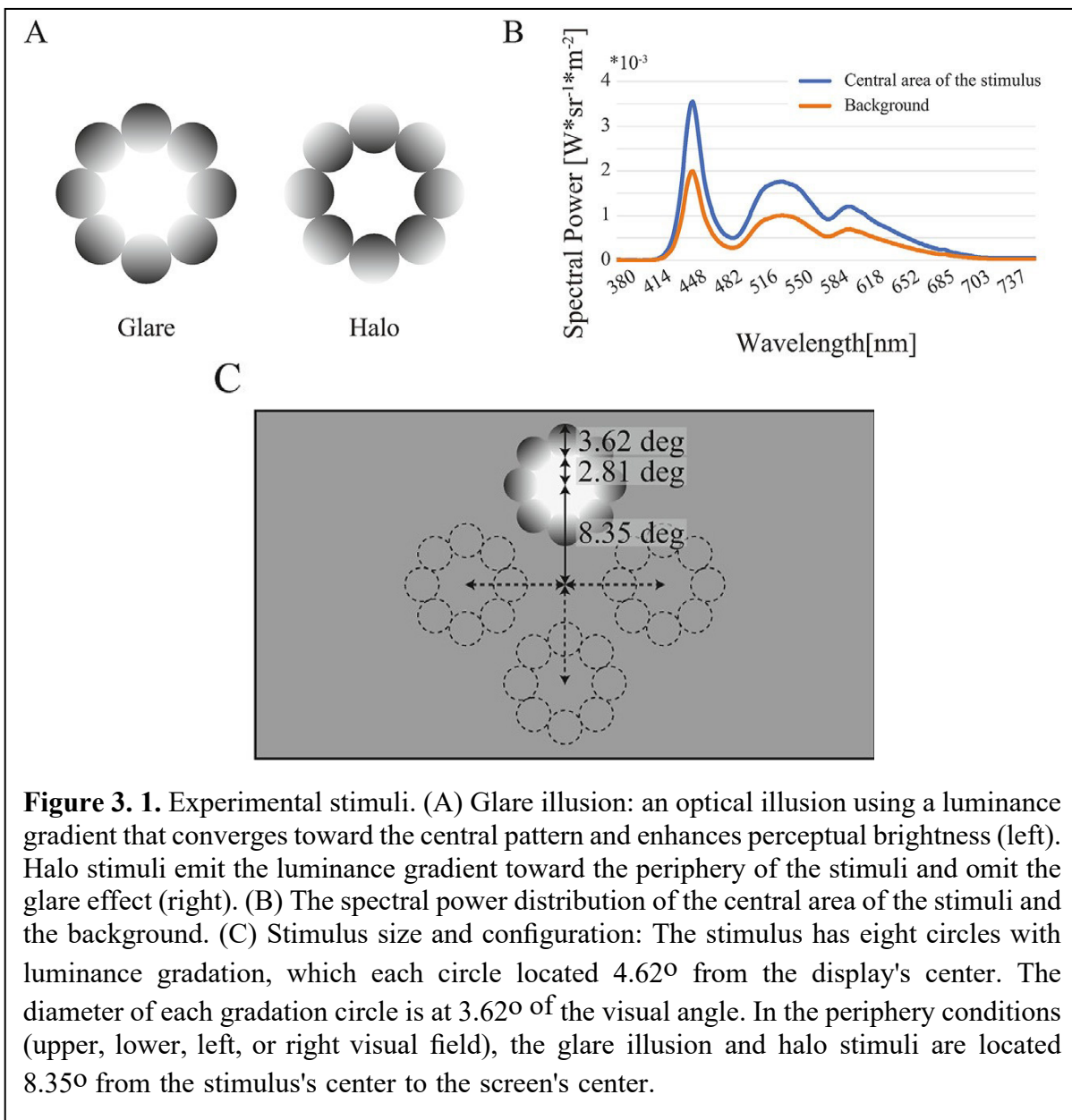
We used the achromatic glare illusion, which had eight circles of luminance gradation converging from the periphery to the center white region of the stimulus (which is a similar design to “phantom illumination” figure [58]). We also used a pattern with a diverging luminance pattern by rotating 180° the same gradient luminance of glare illusion as a control referred to as the halo stimuli (Figure 3.1A) [25], [29]. This particular type of glare/halo stimuli has many advantages compared to the Asahi glare illusion and the ring-shaped glare illusion. The areas of the foveal and peripheral regions in the inverted Asahi glare illusion are not identical. Therefore, adjusting the global luminance of the Asahi glare illusion and its inverted form to the same values would be difficult. In comparison, the ring-shaped glare illusion and its inverted form would result in the same issue as the Asahi glare illusion.

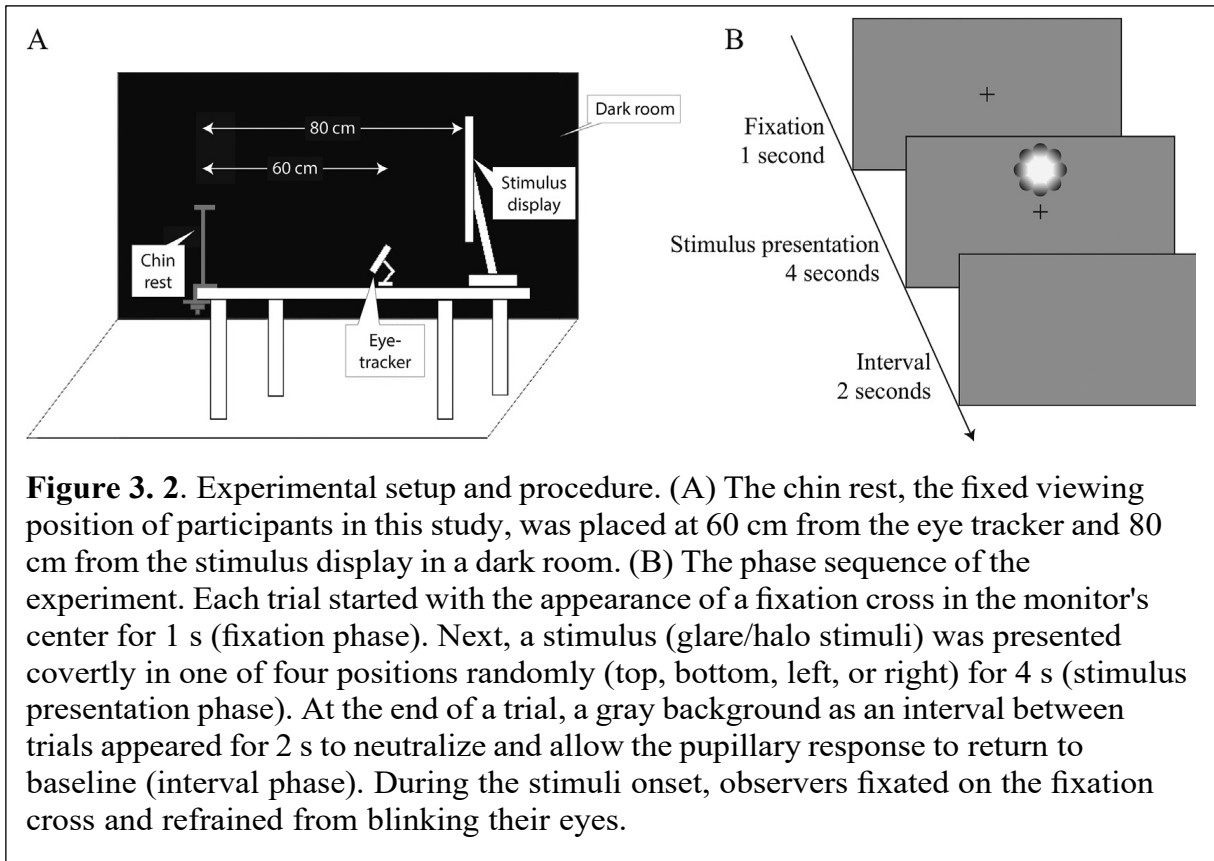
The achromatic points of the stimuli's luminance gradation were 0.2959 and 0.3249 in the CIE1931 color space, while the luminance of Y changed linearly from 0.4218 cd/m² to 93.45 cd/m². The luminance of the background and center white region of the stimuli were 53.30 cd/m² and 93.45 cd/m², respectively. The spectral power distribution of the glare illusion's area and background (Figure 3.1B) was measured by a spectroradiometer (SR-3AR, TOPCON, Tokyo, Japan). The stimulus size and configuration were identical to those used by Suzuki et al. (2019). The center condition (i.e., the stimulus was presented in the center of the VF) contained eight circles with luminance gradation, with each circle located 4.62° from the center of the screen (Figure 3.1C). The diameter of each gradation circle was the visual angle of 3.62°. In the periphery condition (i.e., the stimulus was presented in the upper, lower, left, or right VF), the glare illusion and halo stimuli were located 8.35° from the screen's center, keeping the exact configuration of the stimulus luminance and size as in the center condition. We included a fixation point of 0.1° positioned at the center of the screen in both the center and periphery conditions. Thus, participants looked at the stimuli with their peripheral vision in the

periphery condition. The experiment was conducted using MATLAB R2019b (MathWorks, Natick, MA) and Psychtoolbox [59]. All stimuli were presented on a liquid-crystal display (LCD) monitor (Display, Cambridge Research Systems Ltd., Kent, UK) with a resolution of 1920 1080 pixels and a refresh rate of 120 Hz.

3.5.3 Procedure

Participants rested their chins at a fixed viewing distance of 60 cm from the eye tracker and 80 cm from the stimulus display in a dark room. The experimental setup is described in Figure 3.2A. The eye tracker was in front of and at the center of the LCD display. In addition, the chin rest was placed in front of the eye tracker and was set at the center viewpoint of the





stimulus display. We calibrated the eye tracker using a standard five-point calibration before starting each session. Each trial began with a fixation cross presented on the monitor's center for 1 s. Afterward, the stimuli were randomly presented for 4 s in the upper, lower, left, right, or center area of the screen (Figure 3.2B). Participants were asked to fixate upon the central fixation cross while a stimulus was presented in the screen's periphery. Participants were instructed to refrain from blinking their eyes during the fixation and stimulus presentation periods. A blank screen with no fixation cross or stimulus (interval stage) was presented for 2 s between each trial to neutralize the participants' pupil diameter. The stimulus was repeatedly presented 15 times per condition. Thus, the experiment consisted of 150 trials: 5 VF locations (center, upper, lower, left, and right) 2 stimulus patterns (glare and halo stimuli) 15 trials, divided into two sessions. Participants were provided with a break of about 5 min between sessions.

3.5.4 Pupil recording and analyses

We measured pupil size and eye gaze movements using an eye-tracking system (EyeLink 1000; SR Research, Ontario, Canada) at a sampling rate of 500 Hz. The tracking was based on “pupil diameter” using the centroid mode in the device setting. The device generated pupil data in arbitrary units (pixels) and converted them to z-scores (z) during

the entire experiment (two sessions) for each participant. We used cubic Hermite interpolation for the pupil data during eye blinks, which were obtained as values of zero. The analysis excluded data from trials with additional artifacts, in which the velocity change in pupil size was more than 20 z/s or the average gaze position during the presentation exceeded the radius of 2.81° (i.e., the white area of the stimulus in the center condition). Additionally, we conducted a principal component analysis at each timepoint for pupil size. We rejected trials with a Euclidian distance (calculated using the first and second principal components) exceeding 3σ of all trials. The average rejected trials comprised 4.6% of all trials per participant.

For the baseline correction of pupillary response, the first 0.2 s served as a baseline after the stimulus onset (the baseline period is shown as the dotted line in Figure 3.4), and we subtracted this baseline from any samples recorded after stimulus presentation. Then, the time course of pupillary responses for each VF location and stimulus pattern was averaged across all repeated trials. Next, we calculated early and late components [60], [61] to assess pupillary light reflex (PLR) responses and their “recovery” after the PLR. First, we averaged the pupil responses across all location data with time series for each participant. Second, we computed the pupil slope using second-order accurate central differences to obtain the maximum pupil constriction latency (MPCL). The MPCL was defined as an initial local maximum negative value of the slope separated by 0.25 s (Figure 3.3). The early component was defined by the average pupil data within the window of $MPCL \pm 0.25$ (Figure 3.5A, red shaded area). The late component, defined as the area under the curve (AUC), was computed as follows:

$$AUC = \sum_{i=MPCL}^4 x_i - x_{MPCL} \quad (1)$$

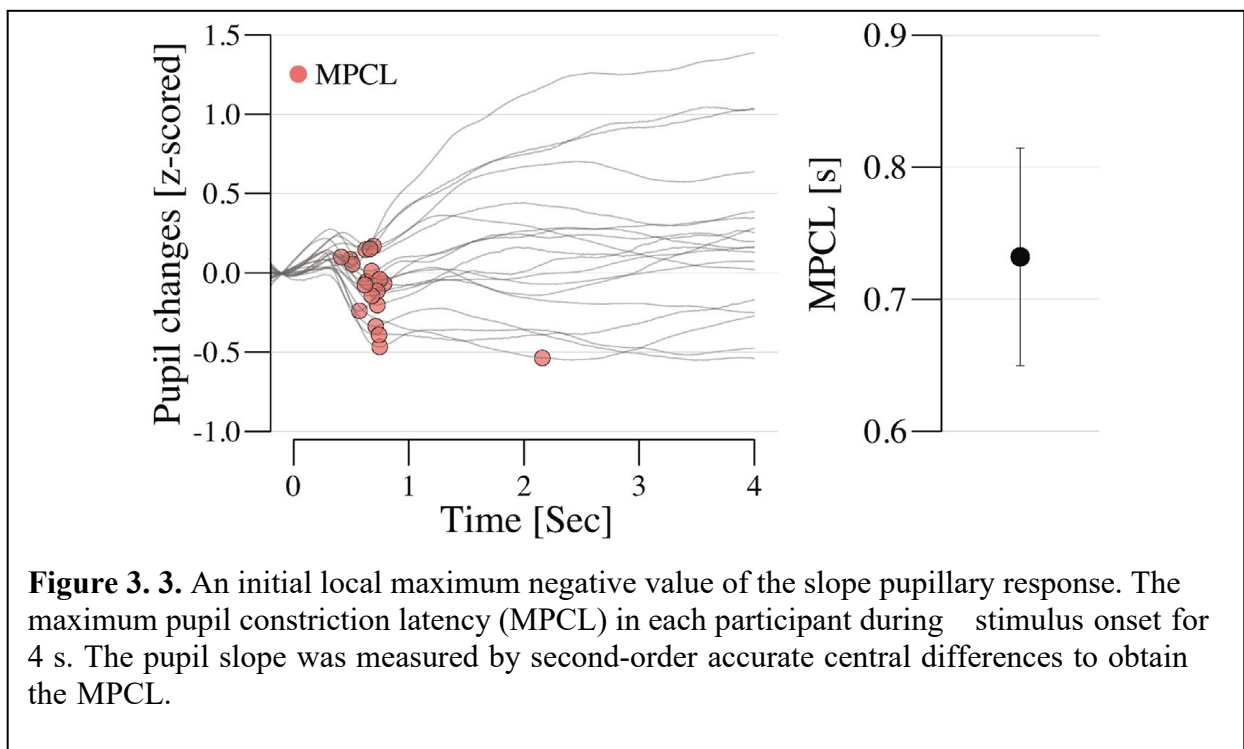
where x represents pupil size at i seconds after stimulus onset. The AUC represents a total pupil diameter increase from the PLR toward baseline pupil size (i.e., a pupil size “recovery” back to baseline).

3.5.5 Statistical analyses

We conducted separate statistical analyses for the center and periphery conditions. A paired-sample t-test was performed on the pupillary response in the center condition. In the periphery conditions, we conducted a two-way repeated-measures analysis of variance (ANOVA) with the effect of 4 VF locations (upper, lower, left, and right) 2

stimulus patterns (halo and glare illusion) on the pupillary response as within-subject factors. We performed Greenhouse–Geisser corrections when the results of Mauchly's sphericity test were significant. Pairwise comparisons of the main effects for multiple comparisons in the periphery conditions were tested by paired-sample t -tests. In the multiple comparisons, p -values were corrected by the Bonferroni–Holm method.

The significance level (α) was set to $p < 0.05$ for all analyses. Effect sizes were given as partial η^2 (η^2) for ANOVA and Cohen's d_z for the paired t -test analysis. We also reported the Bayes factors for estimating the relative weight of the evidence in favor of H_1 over H_0 as BF_{10} for post-hoc pairwise comparisons and t -tests [42]. All statistical analyses were



performed using Jamovi 1.1.9.0 [62], SPSS Statistics for Windows (v26.0; IBM, Armonk, NY) [63], and the BayesFactor package (v0.9.12–4.2) (Morey, 2019) for R (v3.6.3; The R Foundation, Vienna, Austria) [64].

3.6 Results

We observed pupillary responses during the glare illusion or halo stimuli presentation at one out of five VF locations (i.e., upper, lower, left, right, and center), as shown in Figure 3.4. As reported previously [25], [27], [42], we confirmed that the mean pupil size from 0 s to 4 s was significantly constricted by the glare illusion in the center condition ($t(18) = -3.07$, $p = 0.007$, Cohen's $d_z = 0.704$, $BF_{10} = 7.36$). Two-way

repeated measures ANOVA on the pupillary changes in the periphery conditions revealed a significant main effect of stimulus patterns ($F(1, 18) = 5.281, p = 0.034, \eta_p^2 = 0.227, BF_{10} = 1.658$) and VF locations ($F(2.37, 42.654) = 7.438, p = 0.001, \eta_p^2 = 0.292; BF_{10} = 49.048$). However, there was no significant interaction between VF locations and stimulus patterns ($F(2.597, 46.749) = 0.121, p = 0.929, \eta_p^2 = 0.007, BF_{10} = 0.084$).

We first determined the MPCL (0.731 ± 0.361 s) to calculate the early and late components of pupillary response (see Method and Figure 3.3). For the center condition, there were significant differences of early ($t(18) = -2.425, p = 0.026, \text{Cohen's } d_z = 0.556, BF_{10} = 2.372$) and late components ($t(18) = -2.344, p = 0.031, \text{Cohen's } d_z = 0.538, BF_{10} = 2.076$) of pupil response between glare and halo stimuli (Figure 3.5A).

In the early component for the periphery conditions (Fig. 3.5B, Table 3.1), two-way repeated measures ANOVA revealed a significant main effect of stimulus patterns ($F(1, 18) = 8.134, p = 0.011, \eta_p^2 = 0.311; BF_{10} = 5.976$) and VF locations ($F(2.89, 52.023) = 4.356, p = 0.009, \eta_p^2 = 0.195, BF_{10} = 2.918$). However, the post-hoc multiple comparisons for VF locations showed that no pairs of VF locations reached statistical significance ($p > 0.05$, Table 3.2). In addition, there was no significant interaction between VF locations and stimulus patterns (Table 3.3; $F(2.663, 47.936) = 1.066, p = 0.367, \eta_p^2 = 0.056, BF_{10} = 0.232$).

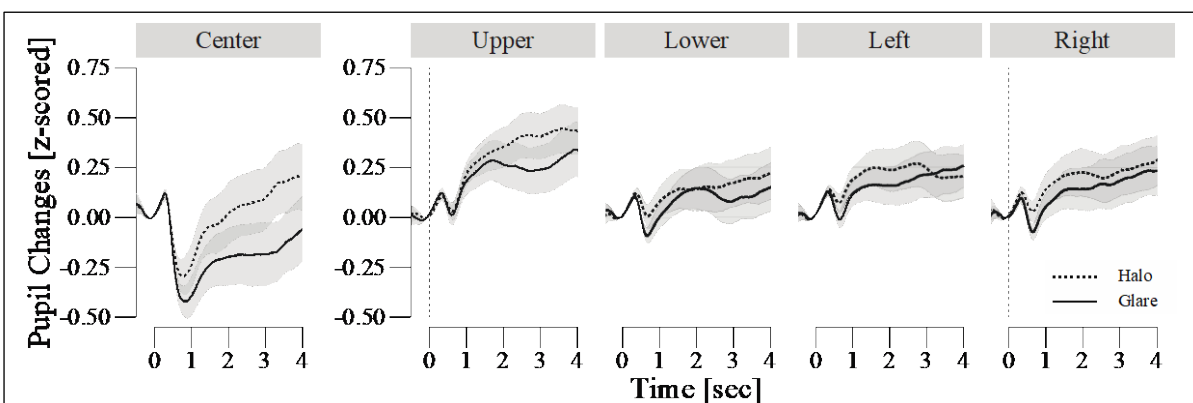


Figure 3. 4. Pupillary changes in five locations (center, upper, lower, left, and right). The average pupil diameter change (z-score) during stimuli onset for 4 s in each position and stimuli (glare and halo stimuli). The shaded areas indicate the standard error of the mean. The dotted lines show the period for the baseline pupillary response (0.2 s).

Table 3. 1. Main effects of analysis of variance in the early component

Factor	df	F	p	sig	η_p^2
Visual field locations	2.890	4.356	0.009	**	0.195
Stimulus patterns	1.000	8.134	0.011	*	0.311
Visual field locations \times Stimulus conditions	2.663	1.066	0.367	ns	0.056

Table 3. 2. Multiple comparisons for visual field locations in the early component

Pair	t	df	p	adj.p	sig	Cohen's d_z
Lower-Left	2.880	18	0.010	0.060	Lower = Left	0.661
Left-Right	2.568	18	0.019	0.060	Left = Right	0.589
Upper-Lower	2.318	18	0.032	0.097	Upper = Lower	0.532
Upper-Right	2.158	18	0.045	0.134	Upper = Right	0.495
Lower-Right	0.521	18	0.609	1.000	Lower = Right	0.120
Upper-Left	0.392	18	0.700	1.000	Upper = Left	0.090

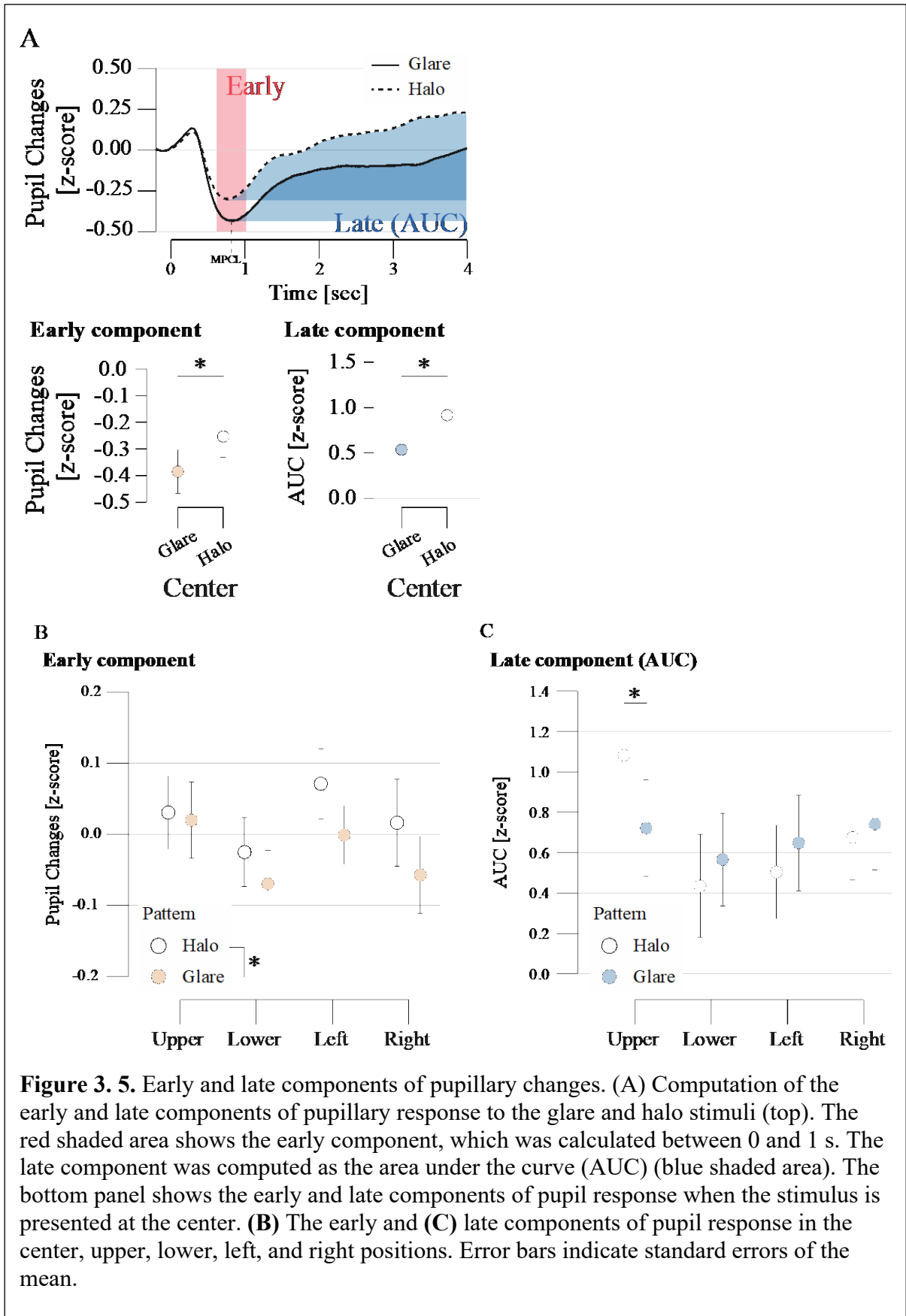


Table 3. 3. Multiple comparisons for the interaction in the early component

Factor	df	F	p	sig	η_p^2
Visual field locations in glare	2.667	3.924	0.017	*	0.179
Visual field locations in halo	2.865	1.392	0.256	ns	0.072
Stimulus patterns in upper	1.000	0.011	0.919	ns	0.001
Stimulus patterns in lower	1.000	3.090	0.096	+	0.147
Stimulus patterns in left	1.000	4.016	0.060	+	0.182
Stimulus patterns in right	1.000	4.216	0.055	+	0.190

In the late component (the AUC) for the periphery conditions, two-way repeated measures ANOVA revealed significant main effects of VF locations ($F(2.128, 38.303) = 6.436, p = 0.003, \eta_p^2 = 0.263, BF_{10} = 70.782$) and VF locations \times stimulus patterns interaction (Fig. 5C and Table 3.4) ($F(2.983, 53.691) = 2.883, p = 0.044, \eta_p^2 = 0.138, BF_{10} = 1.367$). Most importantly, the post-hoc multiple comparisons for the interaction showed that the AUC for the glare illusion was significantly smaller than that in halo stimuli in the UVF ($t(18) = 6.847, p = 0.017, \eta_p^2 = 0.276, BF_{10} = 3.283$) but not in the LVF ($t(18) = 0.13, p = 0.723, \eta_p^2 = 0.007, BF_{10} = 0.252$), left ($t(18) = 0.466, p = 0.503, \eta_p^2 = 0.025, BF_{10} = 0.292$) or right VF ($t(18) = 0.798, p = 0.384, \eta_p^2 = 0.042, BF_{10} = 0.338$) (Table 3.5). Since the AUC was defined as an integral value (see Method) from the PLR to stimulus offset, a smaller AUC indicates a slow recovery of pupil dilation toward the baseline pupil size. The following multiple comparisons for VF locations showed that the UVF produces a larger AUC than the LVF ($t(18) = 2.806, p = 0.035$, Cohen's $d_z = 0.644$), left ($t(18) = 4.091, p = 0.004$, Cohen's $d_z = 0.938$) and right VF ($t(18) = 2.382, p = 0.085$, Cohen's $d_z = 0.547$) (Table 3.6), in line with previous studies [7], [10], [45], [46]. We also found a significant effect of VF locations on the AUC for the halo stimulus ($F(2.533, 45.596) = 7.736, p = 0.001, \eta_p^2 = 0.301$). The post-hoc multiple comparisons for VF locations for the halo stimulus showed that the UVF produces a larger AUC than the left VF ($t(18) = 4.07, p = 0.004$, Cohen's $d_z = 0.934$), right ($t(18) = 3.697, p = 0.005$, Cohen's $d_z = 0.848$) and LVF ($t(18) = 3.388, p = 0.01$, Cohen's $d_z = 0.777$).

Table 3. 4. Main effects of analysis of variance in the late component

Factor	df	F	p	sig	η_p^2
Visual field locations	2.128	6.436	0.003	**	0.263
Stimulus patterns	1.000	0.276	0.605	ns	0.015
Visual field locations \times Stimulus patterns	2.983	2.883	0.044	*	0.138

Table 3. 5. Multiple comparisons for visual field locations in the late component

Pair	t	df	p	adj.p	sig	Cohen's d_z
Upper-Left	4.091	18	0.001	0.004	Upper > Left *	0.938
Upper-Lower	2.806	18	0.012	0.035	Upper > Lower *	0.644
Upper-Right	2.382	18	0.028	0.085	Upper = Right	0.547
Left-Right	1.825	18	0.085	0.254	Left = Right	0.419
Lower-Right	1.761	18	0.095	0.254	Lower = Right	0.404
Lower-Left	0.081	18	0.936	0.936	Lower = Left	0.019

Table 3. 6. Multiple comparisons for the interaction in the late component

Factor	df	F	p	sig	η_p^2
Visual field locations in glare	2.293	0.974	0.396	ns	0.051
Visual field locations in halo	2.533	7.736	0.001	***	0.301
Stimulus patterns in upper	1.000	6.847	0.017	*	0.276
Stimulus patterns in lower	1.000	0.130	0.723	ns	0.007
Stimulus patterns in left	1.000	0.466	0.503	ns	0.025
Stimulus patterns in right	1.000	0.798	0.384	ns	0.042

3.7 Discussion

This study reported pupil size during the glare illusion and halo stimuli presented in five VF locations (upper, lower, left, right, and center). We confirmed that the glare illusion induces enhanced pupillary constriction compared with halo stimuli in the center condition as reported previously [25], [27]. To assess whether there is a lower-, higher-, or combined- (lower- and higher-) level visual processing implication on pupil response to the glare illusion across VF locations, we divided the pupillary data into early and late components. The early and late components of pupillary data allowed us to assess visual processing from the temporal aspects of pupillary change. First, we found that glare-related pupil constrictions were seen in all VFs to the same degree in the center condition in the early stage. Second, VF anisotropy in the pupillary response (i.e., large pupil dilation in response to the stimuli in the UVF) was present in the late component, but not in the early component.

The early stage of the pupillary response reflects the changes in physical light intensity via lower-level visual processing [52], [65]. In addition, some studies discovered that PLR is influenced by subjective brightness perception [25], [27], [38] and visual attention on higher-level visual processing [66]. Along this line, our data seems consistent with the idea that the early component of the pupillary response involves both lower- and higher-level visual processing that creates the increased brightness perception in the glare illusion.

Previous studies have revealed that there are a smaller number of photoreceptors, acuity, and less spatial resolution with decreasing retinal eccentricity in the UVF than in the LVF [67]. Portengen et al. conducted an experiment using pupillometry and flickering stimuli in the vertical hemifield, and they found a pupillary anisotropy effect in which the UVF has greater and more sensitive pupil amplitude changes in the flickering frequency domain than the LVF [9]. In addition, paintings, images, or cartoons depicting the sun-induced greater pupil constriction [17], [27], [68], most likely in response to strong light from the sun. We hypothesized that the effect of pupil changes in response to the stimuli would vary across different maps due to the lower-characteristic asymmetry as well as assumptions that the light source is in the UVF [54], [56]. The current results support the idea that the interaction of lower- and higher-level visual processing of illusory glare perception could appear as the temporal aspects of pupillary response; at the late component, glare-related pupil constrictions were larger in the UVF than in the other VFs. That is, the late component of pupillary responses might be affected by visual acuity, spatial resolution as well as brightness perception.

The visual system processes different contexts of scenes in nature to help humans understand the visual world [69]. Anatomically, sensory input from a varied VF map is processed by different areas of the primary cortex; the signal from the UVF is more dominantly processed in the ventral stream of the visual pathway [70]–[72]. Because of these stream differences, superior cognitive processing in the UVF and LVF depends on the type of cortical processing required for the task [70], [72]. Thus, our results imply that the cortical processing from the ventral portion may involve VF anisotropy in the pupillary response to the glare illusion. This is consistent with the increases in blood-oxygen-level-dependent (BOLD) signals in the occipitotemporal and/or collateral sulcus in response to the glare illusion [73].

The reduced pupil dilation in response to the glare illusion compared with the halo stimuli that only occurred in the UVF may be explained by the dominance of cognitive bias formed by statistical regularity in the processing of natural scenes that can represent a visual image of the UVF. The reduced pupil dilation (i.e., greater pupillary constrictions) may be observed when light sources appear in the VF other than in the UVF since these cases would be somewhat unexpected with an assumption of the light-from-above in the visual system. In the context of cognitive bias formed by statistical regularity in natural scene processing, human vision can often be exposed to light coming from the UVF [48], [54], [56], [74]–[77]. Thus, our finding that vastly reduced pupil dilation occurs in

response to the glare illusion in the UVF may be interpreted as the result of superior cognitive bias formed by statistical regularity in the processing of natural scenes in the UVF. This process may be related to the variable response of pupil size to the probable dazzling effect geared toward preventing incapacitated vision [78].

Our study revealed that stimulus-evoked pupillary dilation and glare-related pupil constriction both point to VF anisotropy. VF anisotropy in pupil responses has been reported in the present study and elsewhere [7], [9], [10], [45], [46]. Apart from the effect of the light-from-above on the reduced pupil dilation discussed in the previous paragraph, the pupillary changes might be controlled by the nature of VF anisotropy, such as visual acuity or spatial frequency sensitivity; we cannot oppose the effect of anisotropy in VFs on pupillary response to the stimuli in each position in the present study. However, we note that our argument was under the assumption that the mechanisms that involve the brightness enhancement in the glare illusion via low- and high-order visual processing relates to the pupillary response since post-hoc multiple comparisons for the interaction exhibited a significant difference between the glare and halo stimuli only in the UVF. We have two limitations of the present study. First, we analyzed the pupillary data in the peripheral condition separately from the center condition, although our experiment designed those conditions within the same block. Thus, the higher luminance of the central white area in the center condition might affect the pupil size in the following trial. Second, another concern is that the pupillary response to the halo stimuli in the UVF might generate pupillary dilation rather than pupil constriction induced by the glare illusion. This phenomenon may be due to the better contrast sensitivity in the lower, left, and right VFs than the UVF [79]. Thus, this effect should affect the pupillary response in both the halo and glare illusion. Therefore, we believe that the differences in pupillary changes between the halo and glare illusion should still be informative. Furthermore, future studies comparing behavioral brightness data and pupillary responses could support the phenomena of higher pupillary sensitivity in UVF.

3.8 Conclusion

This study shows that stimulus-evoked pupillary dilation at the early component and glare-related pupil constriction in the late component occurred only in the UVF. These results indicate that the pupillary response in the glare illusion located at the UVF might relate to low- and higher-level visual processing compared with other VFs. As previously

noted, the UVF's superior specific cognitive processing occurs via a different dominant visual processing stream. This may be clarified by the superior cognitive bias formed by statistical regularity in natural scene processing due to ecological factors, such as the adaptive response to the glare illusion that represents the sun as a dangerous light source. Furthermore, the present finding offers valuable insights on VF anisotropy to reduce the potential glare effect of peripheral VFs experienced in daily vision. These might be applicable in informing architectural, light, and application design of a glare source.

Chapter 4

Paper 3: Brightness perception in world-centered coordinates assessed by pupillometry

4.1 Summary

After conducting the first experiment, the issue was found. The first experiment showed that low- (spatial resolution of attention, visual accuracy, and contrast sensitivity) and higher-order cognition (the cognitive bias formed by statistical regularity in the processing of natural scenes) affected the anisotropy of subjective brightness perception in the peripheral VF. An issue (the possibility that the differences in retinal coordinates and many opponent processes in the human visual system will affect the subjective brightness perception in the VFs) that arises in experiment 1 was overcome by conducting experiment 2 of this thesis project. The underlying methods in experiment 2 by manipulating the world-centered coordinates through *active* (requiring head movement) and *passive scenes* (without head movement) experiments, which are based on the pupillary response to the glare and halo, were performed to attain the second aim (to investigate the anisotropy of subjective brightness perception in world-centered coordinates) of this thesis. A detailed investigation of experiment 2 in this thesis is described in **Paper 3** within this chapter.

In experiment 2, the constricted pupils in response to the stimuli at the bottom location were caused by the bottom location linked to the peripersonal region by Previc (1998). In addition, the stimuli at the top location were perceived as darker than the bottom due to the influence of ecological factors, e.g., the bright sky. Experiment 2 demonstrated anisotropy on subjective brightness perception in the world-centered coordinates due to the extraretinal information influence and the independence of head movement from the pupillary response.

4.2 Paper information

N. Istiqomah, Y. Kinzuka, T. Minami, and S. Nakauchi, "Brightness perception in world-centered coordinates assessed by pupillometry," *Behavioral Sciences*, vol. 13, issue 1, pp. 1-15, 2023. <https://doi.org/10.3390/bs13010060>.

4.3 Abstract

Subjective brightness perception reportedly differs among the peripheral visual fields owing to lower- and higher-order cognition. However, there is still a lack of information associated with subjective brightness perception in the world-centered coordinates, not in the visual fields. In this study, we aimed to investigate the anisotropy of subjective brightness perception in the world-centered coordinates based on pupillary responses to the stimuli in five locations by manipulating the world-centered coordinates through active (requiring head movement) and passive scenes (without head movement) in a virtual reality environment. Specifically, this study aimed to elucidate if there is an ecological advantage in the five different locations in the world-centered coordinates. The pupillary responses to glare and halo stimuli indicated that the brightness perception differed among the five locations in the world-centered coordinates. Furthermore, we found that the pupillary response to stimuli at the top location might be influenced by ecological factors (such as from the bright sky and the sun's existence). Thus, we have contributed to the understanding of the extraretinal information influence on subjective brightness perception in the world-centered coordinates, demonstrating that the pupillary response is independent of head movement.

4.4 Introduction

Different perceptions of an identical object located in the different eye visual fields (VFs) are known as VF anisotropy. VF anisotropy may be evoked by the opponent processes of many neural functions in the visual system. For example, the visual input signals projected onto the retina from the left VF are carried to the right primary visual cortex (visual area 1; V1) and vice versa. Furthermore, in human visual processing, the input signals from V1 are projected to the prestriate cortex (visual area 2; V2) via the ventral stream, representing visual input derived from the natural world.

In terms of a visual input representation, Andersen et al. (1993) proposed that the spatial information's representation is configured by collecting visual stimuli information that is formed by various coordinate transformations during visual processing [80]. Furthermore, visual processing starts when the light rays hit the retina, and visual input signals are encoded in the retinal coordinates. Hereafter, the visual signals (retinal coordinates) are combined with the non-visual signals (extraretinal coordinates) in the brain to encode the visual stimuli. These extraretinal coordinates can be obtained from non-retinal coordinates. For example, first, head-centered coordinates refer to the head frame as the reference defined by integrating the retinal

coordinates and position of the eye. Second, body-centered coordinates can be obtained by combining information regarding retinal, eye, and head positions. Third, world-centered coordinates are formed by collecting information of the head-centered coordinates and vestibular input (information source that senses the rotational movement for spatial updating).

In addition, in most recent studies focusing on perceptual differences among the VFs, the observers' head was fixed, and the gaze was fixated on a reference object placed in the central VF. Many notable reports have been made on VF anisotropy (manipulating retinal coordinates) regarding many aspects of visual perception [1]–[4]. Specifically, the vertical hemifield has a dominant effect among the VFs compared with the horizontal hemifield [5]. Moreover, during psychophysical experiments that require attentional resources in response to a change in the light source, pupil sensitivity to light is higher in the upper visual field (UVF) than in the lower visual field (LVF) [7], [9], [10]. Additionally, objects located in the UVF are biased toward the extrapersonal region (for scene memory), whereas objects in the LVF are biased toward the peripersonal (PrP) region (for visual grasping) in 3D-spatial interactions. Other advantages of the LVF include better contrast sensitivity [81], visual accuracy [82], motion processing [83], [84], and spatial resolution of attention and spatial frequency sensitivity [13]. The LVF bias in processing information about an object is caused by the substantially higher number (60% more) of ganglion cells in the superior hemiretina than in the inferior hemiretina [85], which results in an improved visual performance in the former.

VFs are also known to evoke different brightness perceptions. The perceptual brightness modulation is associated with cognitive factors such as memory and visual experience. This effect has been studied using pupillometry, with photographs and paintings of the sun as the stimuli. Binda et al. (2013) confirmed that sun photographs yielded a greater constriction of the pupils than did other stimuli despite physical equiluminant (i.e., squares with the same mean luminance as each sun photograph, phase-scrambled images of each sun photograph, and photographs of the moon) [17]. Subsequently, Castellotti et al. (2020) discovered that paintings including a depiction of the sun produce greater pupil constriction than paintings that include a depiction of the moon or no depiction of a light source, despite having the same overall mean luminance [18]. Recently, Istiqomah et al. (2022) reported that pupillary response to the image stimuli perceived as the sun yielded larger constricted pupils than those perceived as the moon under average luminance-controlled conditions [19]. Their results indicated that perception has a dominant role rather than a mere physical luminance of the image stimuli due to the influence of ecological factors such as the existence of the sun. All of these studies demonstrate that pupillometry reflects not just the physical luminance (low-order cognition) but also the

subjective brightness perception (higher-order cognition) in response to the stimuli. In addition, the previous study by Tortelli et al. (2022) confirmed that pupillary response was influenced by contextual information (such as from the sun's images) considering the differences of inter-individual differences in the observer's perception [86].

Pupillometry is a metric used to measure pupil size in response to stimuli and may reflect various cognitive states. The initial change in pupil diameter is caused by the pupillary light reflex (PLR). However, the degree of change in pupil diameter is influenced by visual attention, visual processing, and the subjective interpretation of brightness. For example, Laeng and Endestad (2012) reported that a glare illusion conveyed brighter than its physical luminance induced greater constricted pupils [27]. This glare illusion has a luminance gradient converged toward the pattern's center that enhances the brightness intensely [25], [87]. Furthermore, Laeng and Sulutvedt (2014) revealed that, owing to the response of the eyes to hazardous light (such as sunshine), the pupils considerably constricted when the participant imagined a sunny sky or the face of their mother under the sunlight [23]. Other previous study by Mathôt et al. (2017) revealed that words conveying a sense of brightness yielded a greater constriction of pupils than those conveying a sense of darkness [24]. These differences indicated the pupils' response to a source that may damage the eyes despite only occurring in the observer's imagination. In addition, Suzuki et al. (2019) revealed that the pupillary response to the blue glare illusion generated the largest pupil constrictions, reporting that blue is a dominant color in the human visual system in natural scenes (e.g., the blue sky) and indicating that, despite the average physical luminance of glare and control stimuli being identical, pupillary responses to the glare illusion reflect the subjective brightness perception [25].

Recently, we demonstrated that the pupillary response to glare and halo stimuli differed depending on whether the stimuli were presented in the upper, lower, left, or right VFs by manipulating the retinal coordinates [35]. We found that pupillary responses to the stimuli (glare and halo) in the UVF resulted in the largest pupil dilation and significantly reduced pupil dilation, specifically in response to the glare illusion due to higher-order cognition. The previous results reflect that the glare illusion was a dazzling light source (the sun) influencing the pupillary responses. However, our previous study and other studies regarding the subjective brightness perception analysis in the VFs (also mentioned in paragraph 3) raise the possibility that the differences in retinal coordinates and many opponent processes in the human visual system will affect the subjective brightness perception in the VFs. Therefore, clarifying whether there is anisotropy of subjective brightness perception by maintaining identical retinal coordinates and manipulating the world-centered coordinates could provide valuable insights

into the anisotropy of subjective brightness perception in the world-centered coordinates based on pupillary responses to the glare illusion and halo stimuli. Particularly, this study aimed to elucidate whether there is an ecological advantage in five different locations in the world-centered coordinates based on pupillary responses to the glare illusion overtly that conveys a dazzling effect.

The difference between our previous and present studies is the visual input, which used the retinal coordinates manipulation in our previous study, and world-centered coordinates (formed by collecting information of the head-centered coordinates and vestibular input) manipulation in this work. To investigate the anisotropy of subjective brightness perception in the world-centered coordinates, we presented the glare and halo as stimuli in five different locations (top, bottom, left, right, and center) in the world-centered coordinates based on the pupillary responses to the stimuli (glare and halo) while the observers fixated on a fixation cross located in the middle of the stimulus. We used a virtual environment to easily control the physical luminance of the stimuli and the designated environment. In addition, the contextual cues of the 3D virtual environment provide more cues of features associated with the given tasks and advantages in decreasing the visual perception area; thus, the observers would perceive the stimuli easily [88]. Furthermore, to form the world-centered coordinates, adding vestibular input to be combined with head-centered coordinates (retinal coordinates and eye position integration) is required. Therefore, we adopted an active scene that instructed the observers to move their heads in accordance with the stimulus' location in the world-centered coordinate as the vestibular input. To ensure that the present study's results are not merely pupil size artifacts induced by the head movement during the active scene, we manipulated the scene by automatically moving the virtual environment as the substance of the head movement in the active scene, called the passive scene, which did not allow the head movement during the stimulus presentation. In addition, we also applied glare as the stimuli and halo manipulation as the stimuli to find out whether there is any distinction between pupillary responses to the glare and halo stimuli, particularly, associated with ecological factors, as the representation of the sun [25], [35], in five locations in the world-centered coordinates. In the present study, through an active and passive scene, we hypothesized that there is anisotropy in the pupillary responses in the world-centered coordinates; particularly, the results would generate the highest difference between pupillary responses to the glare (more constrict than halo) and halo stimuli at the top, and pupillary responses to the stimuli at the top would yield the highest degree of pupillary constriction as a consequence of ecological factors such as avoiding the dazzling effect of sunshine entering the retina.

4.5 Materials & Methods

4.5.1 Participants

A total of 20 participants (15 men and 5 women, aged between 23 and 35 years; mean age = 27.1 and SD = 4.04 years) participated in this study. Two observers' data regarding the change in pupil size were excluded from the analyses as the trial rejection ratio did not exceed 30% after interpolation and filtering in the pre-processing stage. All participants had a normal or corrected-to-normal vision. All experimental procedures were conducted according to the ethical principles outlined in the Declaration of Helsinki and approved by the Committee for Human Research at our university. The experiment was conducted with complete adherence to the approved guidelines of the committee. Written informed consent was obtained from the participants after procedural details had been explained to them.

4.5.2 Stimuli and apparatus

We conducted two experiments on each observer, i.e., the active and passive scenes in the VR environment. We used Tobii Pro VR Integration, which has an eye-tracker installed in HTC Vive head mounted display (HMD), to present the stimuli. We measured pupil diameter and eye gaze movements using an infrared camera at a sampling rate of 90 Hz. As the output, the device produced pupil diameter in meter. We developed the VR environment by using the Unity version 2018.4.8f1 game engine. The HTC Vive HMD has a total resolution of 2160×1200 pixels on two active-matrix organic light-emitting diode screens and a 110° field of view.

The pupil size data measured by the Tobii Pro were transferred to Unity to be saved and processed with the stimulus presentation data. The observer's location in the VR environment was in the center of the gray-grid-sphered background developed in Blender 2.82 software (open-source software for 3D computer graphics). The gray-grid-sphered background was used to provide a sign that the VR environment moved when the observer moved their head.

Moreover, we conducted two experiments through the active scene, in which the observer needed to move their head according to the location of the stimulus in the VR environment, and the passive scene, in which the observer needed to keep their head stable during the experiment. For the passive scene, we recorded the head movement coordinates of four people in a preliminary study using the HTC Vive Pro Eye HMD with an identical VR environment and refresh rate of 90 Hz. Each recording was played to the participants as a replacement for their head movements. By reproducing the head movement coordinates, the VR environment moved automatically according to the location of the stimuli during the experiment. Detailed information on the flow of the experiments is presented in the Procedure subsection.

An achromatic glare illusion (Figure 1A), in which the luminance gradation increases from the periphery to the central white region, and a halo stimulus (Figure 1B), in which the luminance gradation diverges from the periphery to the center, were presented as the stimuli in this study. We used these types of illusion because they have many advantages over the Asahi and ring-shaped glare illusions [35], such as easily distributing the stimulus' physical luminance evenly in the retina compared with the Asahi and ring-shaped glare illusions, creating its inverse form, and ensuring that the average physical luminance between the glare and its inverse form (halo) was the same. In the gray-grid-sphered background, we used the RGB colors [130, 130, 130] and [100, 100, 100] for the gray circle and fixation cross, respectively. Furthermore, for the unit of detailed stimuli and VR environment, we used the Unity unit (one Unity unit identical to one meter). The distance between the participant and the stimulus in the VR environment was 100 m. The stimuli comprised eight luminance gradation circles, each positioned with its center 14.41 m from the center of the stimulus (approximate visual angle of 8.24°), and each gradation circle's diameter was 11.19 m (approximately 6.40°). The central white area of the stimulus was 17.62 m in diameter (approximately 10.07°). Therefore, the overall stimulus diameter was 40 m (approximately 22.62°). The fixation cross was 2.93 m in diameter (approximately 1.68°). The stimuli presented at the VR environment's top, bottom, left, and right were tilted 76.64 m from the central position (approximately 65°). In addition, we analyzed the pupillary size data using MATLAB R2021a.

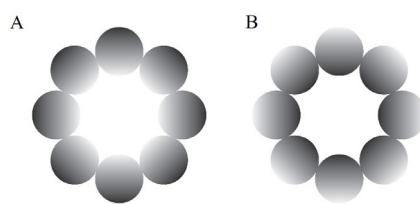


Figure 4. 1. Experimental stimuli. (A) The glare illusion, with an increasing luminance gradation from the periphery to the central white region; (B) the halo stimulus, with a decreasing luminance gradation from the periphery to the center.

4.5.3 Procedure

We were able to produce the same retinal coordinates through the active and passive scenes by placing the stimulus in the five locations of the VR environment and instructing the observer to fixate their gaze on the fixation cross located in the stimulus center, corresponding to world-centered coordinates. In the active scene, participants were required to move their

heads, whereas, in the passive scene, the recording of head movement coordinates displaced the head movement toward the stimulus location. We measured the pupil diameter in response to the stimuli in accordance with the stimulus' location during the stimuli presentation. Both experiments (active and passive) were conducted with the observer in the sitting position and facing forward. The experiments were conducted on different days randomly to prevent eye fatigue caused by the first experiment from influencing the pupillary response in the second experiment. We calibrated the integrated eye tracker on the HMD by performing a standard, five-point calibration before the beginning of each session. In the active scene, each trial started with a direction text presentation of the stimulus locations, appearing in the center of the observer's VF. The observer was instructed to move their head in the direction indicated by the text prompt (top, bottom, left, right, or center, in random order), where they would find the fixation cross. After fixating on the fixation cross for two seconds, the observer was presented with a random stimulus (glare or halo), and the fixation cross remained in the center of the stimulus for four seconds. In the next stage, a gray circle appeared for two seconds to neutralize the observer's pupil size. The observer had to keep their head stable until the gray circle disappeared. Thereafter, the observer reoriented their head to face forward. The procedure for the passive scene was the same as that for the active scene, except that the observer was instructed not to move their head, as the VR environment would automatically move in the direction indicated by the text prompt by playing the recording of the preliminary study (see the Stimuli and apparatus subsection). Details of the procedures in the present study are provided in Figure 2. In each experiment, each stimulus (glare and halo) was presented 15 times per location (top, bottom, left, right, and center). Thus, each experiment consisted of 150 trials (5 locations \times 2 gradient patterns \times 15 trials), including two breaks of approximately 15 min each, and the session after the break started with the eye-tracker calibration.

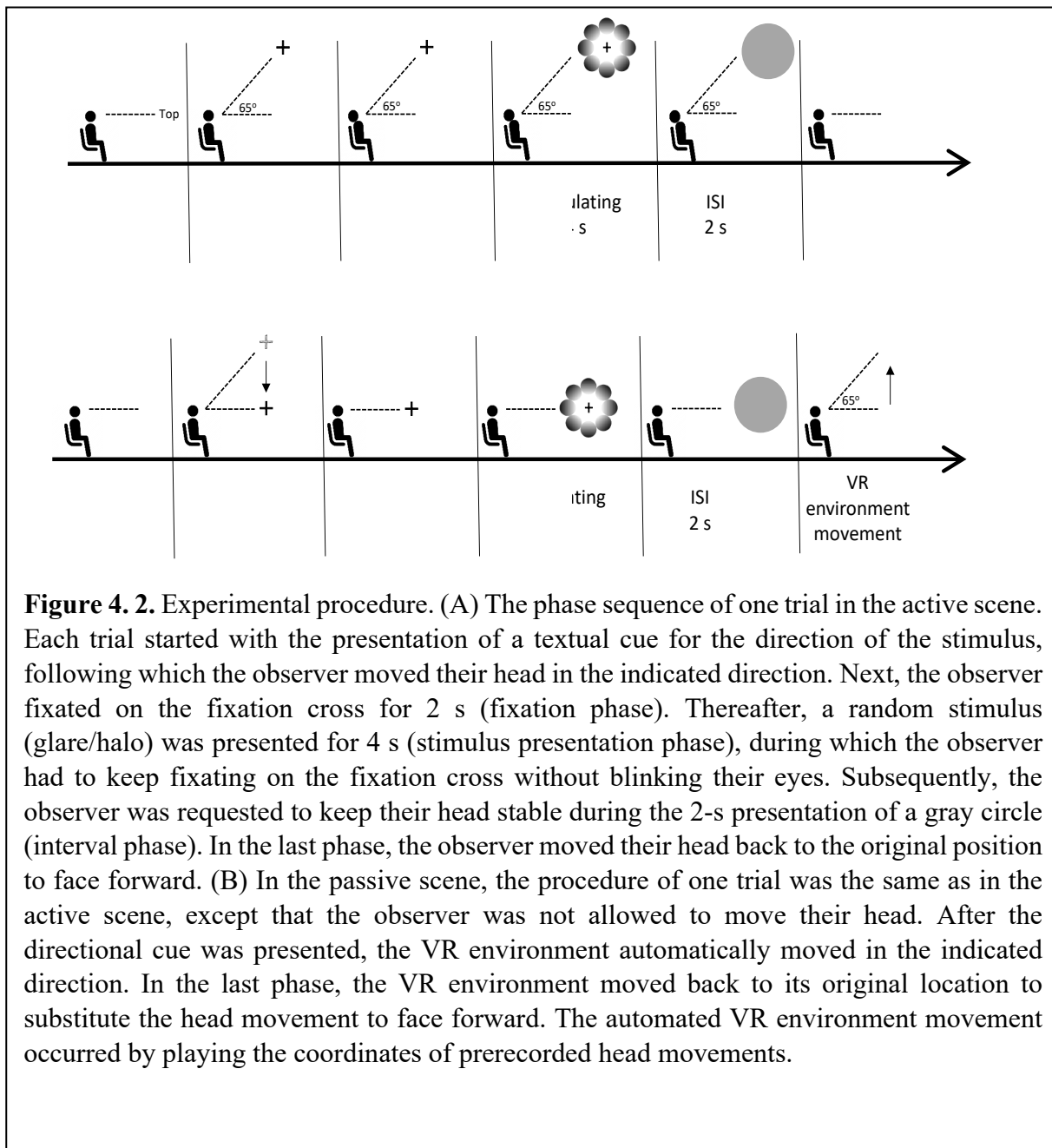


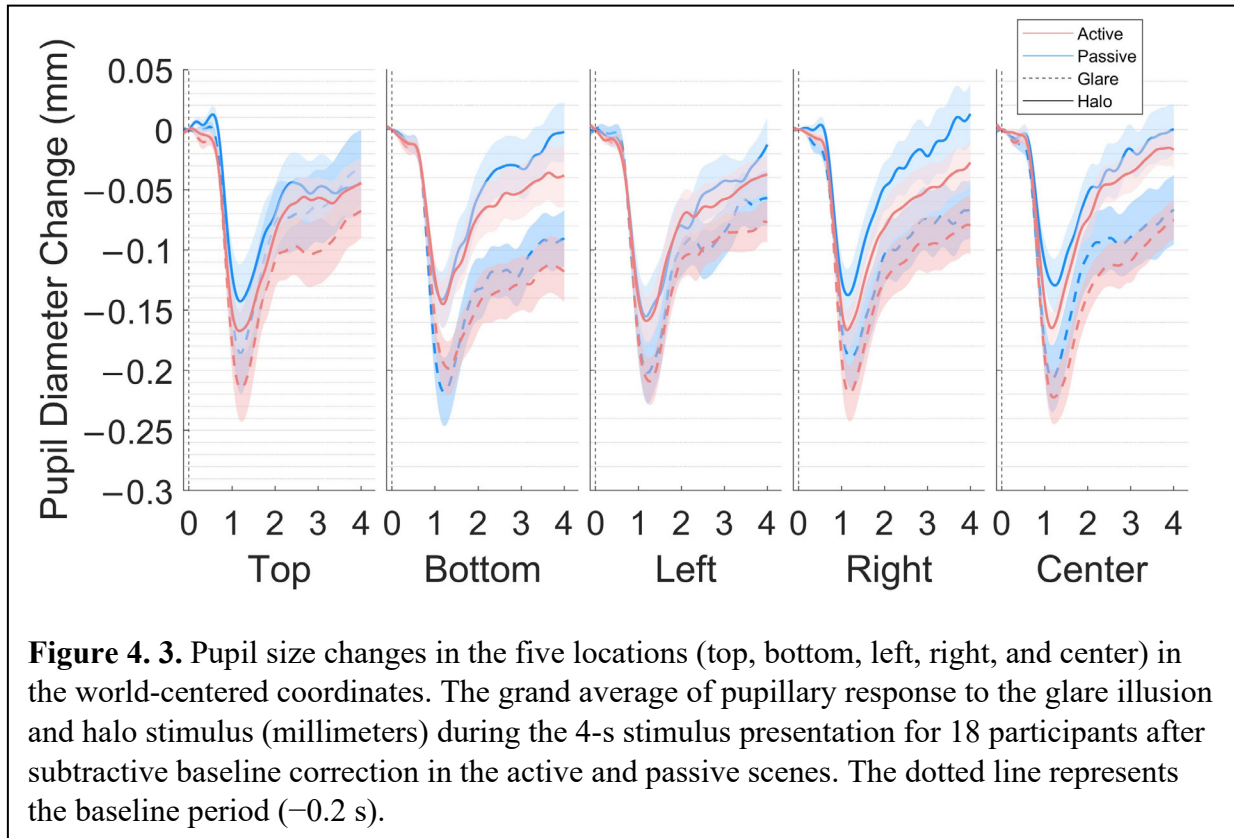
Figure 4. 2. Experimental procedure. (A) The phase sequence of one trial in the active scene. Each trial started with the presentation of a textual cue for the direction of the stimulus, following which the observer moved their head in the indicated direction. Next, the observer fixated on the fixation cross for 2 s (fixation phase). Thereafter, a random stimulus (glare/halo) was presented for 4 s (stimulus presentation phase), during which the observer had to keep fixating on the fixation cross without blinking their eyes. Subsequently, the observer was requested to keep their head stable during the 2-s presentation of a gray circle (interval phase). In the last phase, the observer moved their head back to the original position to face forward. (B) In the passive scene, the procedure of one trial was the same as in the active scene, except that the observer was not allowed to move their head. After the directional cue was presented, the VR environment automatically moved in the indicated direction. In the last phase, the VR environment moved back to its original location to substitute the head movement to face forward. The automated VR environment movement occurred by playing the coordinates of prerecorded head movements.

4.5.4 Pupil and eye gaze analyses

We used cubic Hermite interpolation for the pupil, and eye gaze data during eye blinks displayed as “NaN” values for the pupil data and zero values for the gaze data. Thereafter, we applied the subtractive baseline correction by calculating the mean of 0.2 s pupillary responses before the stimulus onset to define the baseline and subtracting the pupil size from the baseline in each trial (the dotted line in Figure 3 represents the baseline period). Furthermore, a low-pass filter for data smoothing with a 4-Hz cut-off frequency was implemented, as in a previous study [89]. The analysis excluded data from trials with additional artifacts, calculated by thresholding

the peak changes on the velocity of change in pupil size (more than 0.001 mm/ms). In addition, the trials were rejected with a Euclidian distance (calculated using the first and second principal components) exceeding 3σ of all trials. After that, we also rejected the trials if the average of eye gaze fixation during the stimuli presentation exceeded the radius of 5.035° (i.e., the central white area of the stimulus). In the last stage of preprocessing data, we rejected two participants due to the rejected trials ratio exceeding 30%. The average rejection ratios were 14.20% and 1.7% of all trials per observer in the active and passive scenes, respectively. We applied this preprocessing procedure to pupil and eye gaze data.

In addition, for pupil diameter data, we separated the data into two approaches, early and late components [35], [90], [91].



(1) The early component reflected pupillary responses modulated by the physical luminosity of the stimuli via low-order cognition. First, we calculated the pupil slope using second-order accurate central differences to attain the maximum pupil constriction latency (MPCL) of the series data from the beginning of the stimulus presentation until 1 s, which accommodated the large pupil diameter change triggered by the PLR, in each trial and participant (the exact procedure with our previous work to obtain MPCL values, [35]). Thereafter, we grand averaged the pupil data using the following function: $\overline{X}_{MPCL \pm 0.1}$, where x

shows the pupil size at approximately 0.1 s before and after the MPCL as the early component (in millimeters, mm).

(2) The late component (using area under curve, AUC) was significantly influenced by emotional arousal as well as subjective brightness perception via higher-order cognition [25,28,29]. Furthermore, the late component represented the pupil diameter in more time to come back to its initial state, which was calculated as follows:

$$AUC = \sum_{i=MPCL}^4 x_i - x_{MPCL} \quad 1)$$

where x represents the pupil diameter at i seconds when the MPCL occurred until stimulus offset at 4 s. We applied this function to all series data of pupil size in each trial and observer. In the last step, we grand-averaged the size data across the trials and observers for each stimulus pattern and location (in the unit of mm).

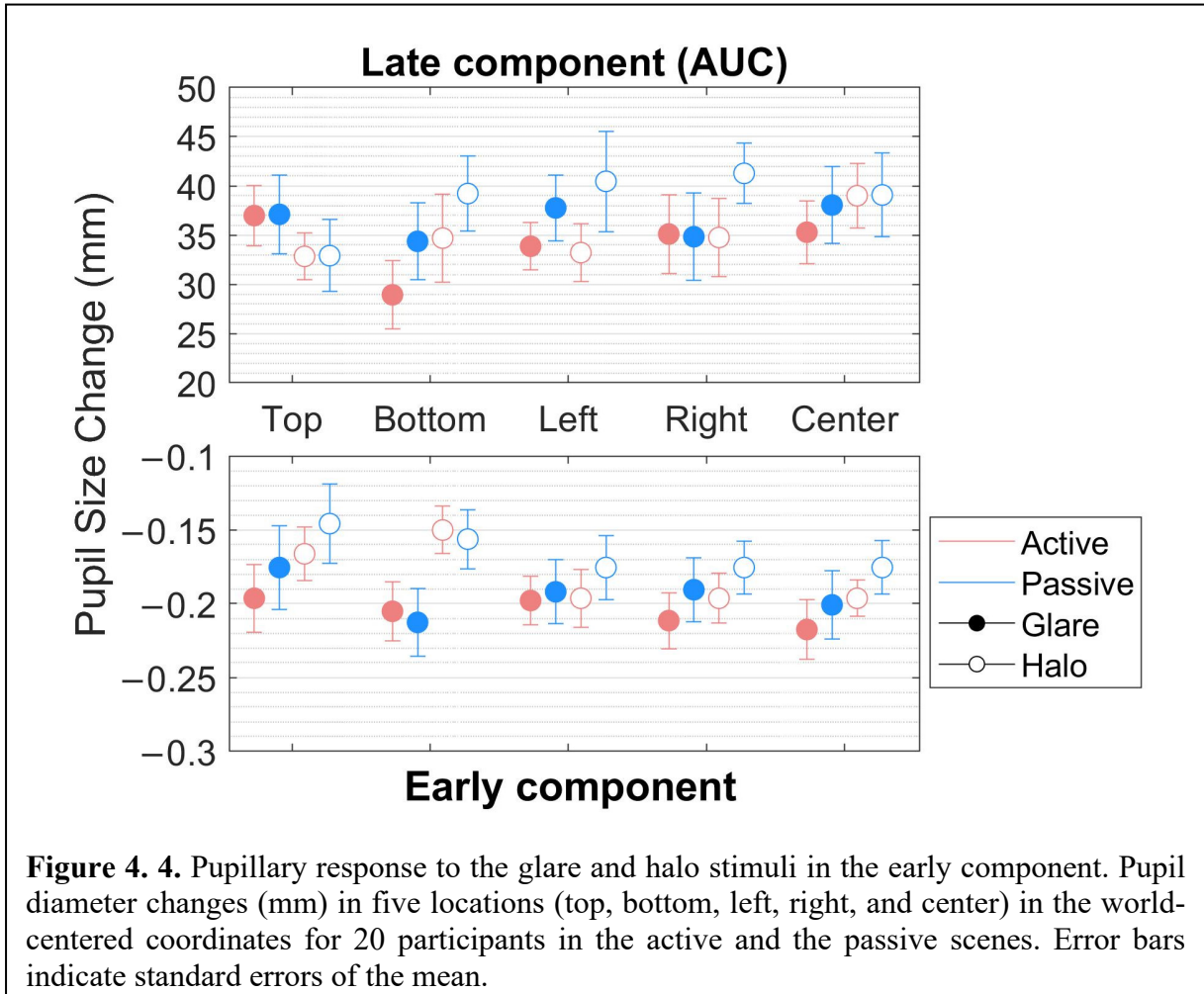
4.5.5 Statistical analyses

We used three-way repeated-measures (rm) analysis of variance (ANOVA) to compare the pupillary responses and y-axes of eye gaze data between the active and passive scenes. The rmANOVA conditions were as follows: two scenes (active and passive), five stimulus locations (top, bottom, left, right, and center), and two stimulus patterns (glare illusion and halo stimulus). We used Greenhouse–Geisser correction when Mauchly’s sphericity test revealed significant differences between the variances of the differences. For the main effect and post-hoc pairwise comparisons, p-values were corrected with the Holm–Bonferroni method, and the resultant significance level (α) was set at <0.05 for all analyses. Cohen’s d and the partial η^2 (η_p^2) were used to represent effect sizes [92]. All statistical analyses were performed using JASP version 0.16.4.0 software [93]. Additionally, we also performed a Bayesian rmANOVA analysis using JASP with default priors, and the BFM and BF10 represent the effect in the model comparison and post hoc comparison by only considering ‘matched models’ due to a more conservative assessment than ‘across all models’, and ‘compared to best model’ as the ‘Order’ [94]. We used the recommendation of Jeffreys (1961) as the guidelines for Bayes factor interpretation [94].

4.6 Results

The main results of the present study are presented as the pupil size and y-axis of eye gaze in response to the glare and halo stimuli for four seconds across the five locations in each scene. The time courses of the pupillary responses to each stimulus pattern (glare and halo),

stimulus location (top, bottom, left, right, and center), and scene (active and passive) are illustrated in Figure 3 (4-s exposure). We separated the pupil size data, based on the MPCL value), i.e., early and late components (Figure 4).



(1) In the early component (Figure 4, bottom), within the range of around 0.1 s before and after MPCL value, an rmANOVA of the pupillary response to the stimuli revealed very strong evidence for the presence of stimulus pattern ($F[1,17] = 58.899, p < 0.001, \eta_p^2 = 0.776, BF_M = 90.205$) but not of the scene, location, and no interaction effect between the parameters (scene, stimulus pattern, and location) (Tables 1 and 2).

Table 4. 1. The main effect of three-way rmANOVA in the early component

Effects	df	F	p	η_p^2
scene	1.000	0.034	0.855	0.002
pattern	1.000	58.899	<0.001	0.776
location	2.430	2.103	0.126	0.110
scene \times pattern	1.000	1.368	0.258	0.074
scene \times location	2.931	2.003	0.127	0.105

pattern \times location	2.677	0.810	0.483	0.045
scene \times pattern \times location	3.064	0.483	0.700	0.028

Table 4. 2. Model comparison using Bayesian rmANOVA in the early component

Models	P(M)	P(M Data)	BF _M	BF ₁₀	Error %
pattern	0.053	0.834	90.205	1.000	
Scene + pattern	0.053	0.121	2.483	0.145	2.028
Scene + pattern + Scene \times pattern	0.053	0.027	0.493	0.032	2.595
pattern + location	0.053	0.015	0.279	0.018	1.753
Scene + pattern + location	0.053	0.002	0.041	0.003	1.875
Scene + pattern + location + Scene \times pattern	0.053	4.728×10^{-4}	0.009	5.672×10^{-4}	2.286
pattern + location + pattern \times location	0.053	3.294×10^{-4}	0.006	3.951×10^{-4}	2.715
Scene + pattern + location + Scene \times location	0.053	7.812×10^{-5}	0.001	9.371×10^{-5}	2.651
Scene + pattern + location + pattern \times location	0.053	4.981×10^{-5}	8.966×10^{-4}	5.975×10^{-5}	4.499
Scene + pattern + location + Scene \times pattern + Scene \times location	0.053	1.853×10^{-5}	3.335×10^{-4}	2.223×10^{-5}	9.561
Scene + pattern + location + Scene \times pattern + pattern \times location	0.053	1.152×10^{-5}	2.074×10^{-4}	1.382×10^{-5}	8.862
Scene + pattern + location + Scene \times location + pattern \times location	0.053	1.628×10^{-6}	2.930×10^{-5}	1.953×10^{-6}	2.833
Scene + pattern + location + Scene \times pattern + Scene \times location + pattern \times location	0.053	3.526×10^{-7}	6.346×10^{-6}	4.229×10^{-7}	3.111
Scene + pattern + location + Scene \times pattern + Scene \times location + pattern \times location + Scene \times pattern \times location	0.053	1.671×10^{-8}	3.008×10^{-7}	2.004×10^{-8}	3.190
Null model (incl. subject)	0.053	1.534×10^{-8}	2.761×10^{-7}	1.840×10^{-8}	1.172
Scene	0.053	2.205×10^{-9}	3.969×10^{-8}	2.645×10^{-9}	2.138
location	0.053	2.526×10^{-10}	4.547×10^{-9}	3.030×10^{-10}	1.397
Scene + location	0.053	3.690×10^{-11}	6.643×10^{-10}	4.427×10^{-11}	1.888
Scene + location + Scene \times location	0.053	1.153×10^{-12}	2.076×10^{-11}	1.384×10^{-12}	2.079

(2) In the late component (the area under the curve [AUC]) (Figure 4, top), defined as integral values of pupillary responses from MPCL value to the end of the stimulus presentation, three-way rmANOVA revealed strong evidence for the presence of the stimulus patterns ($F[1,17] = 12.437$, $p = 0.003$, $\eta_p^2 = 0.423$, $BF_M = 26.005$), and a significant main effect on location ($F[2.944,50.044] = 3.469$, $p = 0.023$, $\eta_p^2 = 0.169$, $BF_M = 0.019$) (Tables 3 and 4). Nevertheless, the post hoc comparisons on location (from the classical frequentist), the Bayesian rmANOVA on location, and other conditions neither show a significant effect. Moreover, further investigation on the post hoc comparison of location from Bayesian analysis obtained moderate evidence only in pairs of top-bottom ($t[18] = 2.586$, $p = 0.192$, Cohen's $d = 0.312$, $BF_{10,U} = 6.660$) and bottom-left ($t[18] = -2.927$, $p = 0.094$, Cohen's $d = -0.251$, $BF_{10,U} = 3.469$). Additionally, we plotted the descriptive information of Bayesian rmANOVA (Figure

5), and the results indicated that the pupillary response to the stimuli at the bottom location has the smallest mean of pupil size change in AUC compared with other conditions.

Table 4. 3. The main effect of a three-way rmANOVA in the late component

	df	<i>F</i>	<i>p</i>	η_p^2
scene	1.000	0.268	0.612	0.016
pattern	1.000	12.437	0.003	0.423
location	2.944	3.469	0.023	0.169
scene × pattern	1.000	0.194	0.665	0.011
scene × location	2.509	1.183	0.323	0.065
pattern × location	2.370	1.551	0.222	0.084
scene × pattern × location	3,476	0.381	0.795	0.022

Table 4. 4. Model comparison using Bayesian rmANOVA in the late component

Models	P(M)	P(M Data)	BF _M	BF ₁₀	Error %
pattern	0.053	0.591	26.005	1.000	
Scene + pattern	0.053	0.243	5.767	0.411	3.596
pattern + location	0.053	0.072	1.390	0.121	2.012
Scene + pattern + Scene × pattern	0.053	0.039	0.729	0.066	2.610
Scene + pattern + location	0.053	0.029	0.534	0.049	2.257
Null model (incl. subject)	0.053	0.010	0.174	0.016	1.546
Scene + pattern + location + Scene × pattern	0.053	0.005	0.093	0.009	3.534
Scene	0.053	0.004	0.065	0.006	1.794
pattern + location + pattern × location	0.053	0.003	0.053	0.005	2.218
Scene + pattern + location + Scene × location	0.053	0.002	0.043	0.004	30.011
Scene + pattern + location + pattern × location	0.053	0.001	0.022	0.002	2.722
location	0.053	0.001	0.019	0.002	1.607
Scene + location	0.053	4.200×10^{-4}	0.008	7.107×10^{-4}	2.787
Scene + pattern + location + Scene × pattern + Scene × location	0.053	3.108×10^{-4}	0.006	5.260×10^{-4}	6.270
Scene + pattern + location + Scene × pattern + pattern × location	0.053	2.234×10^{-4}	0.004	3.781×10^{-4}	6.914
Scene + pattern + location + Scene × location + pattern × location	0.053	6.962×10^{-5}	0.001	1.178×10^{-4}	3.157
Scene + location + Scene × location	0.053	2.189×10^{-5}	3.940×10^{-4}	3.704×10^{-5}	1.888
Scene + pattern + location + Scene × pattern + Scene × location + pattern × location	0.053	1.308×10^{-5}	2.354×10^{-4}	2.213×10^{-5}	9.265
Scene + pattern + location + Scene × pattern + Scene × location + pattern × location + Scene × pattern × location	0.053	6.316×10^{-7}	1.137×10^{-5}	1.069×10^{-6}	3.348

Finally, we conducted a three-way rmANOVA (5 locations × 2 stimulus patterns × 2 scenes) on the y-axis of the eye gaze data to verify that the retinal coordinates were identical across the stimulus locations and patterns between the scenes. We found moderate evidence in favor of the stimulus patterns ($F[1,17] = 4.195$, $p = 0.056$, $\eta_p^2 = 0.198$, $BF_M = 6.845$) (Tables 5 and 6). However, there was neither evidence in the post hoc comparison of stimulus patterns in the Bayesian rmANOVA.

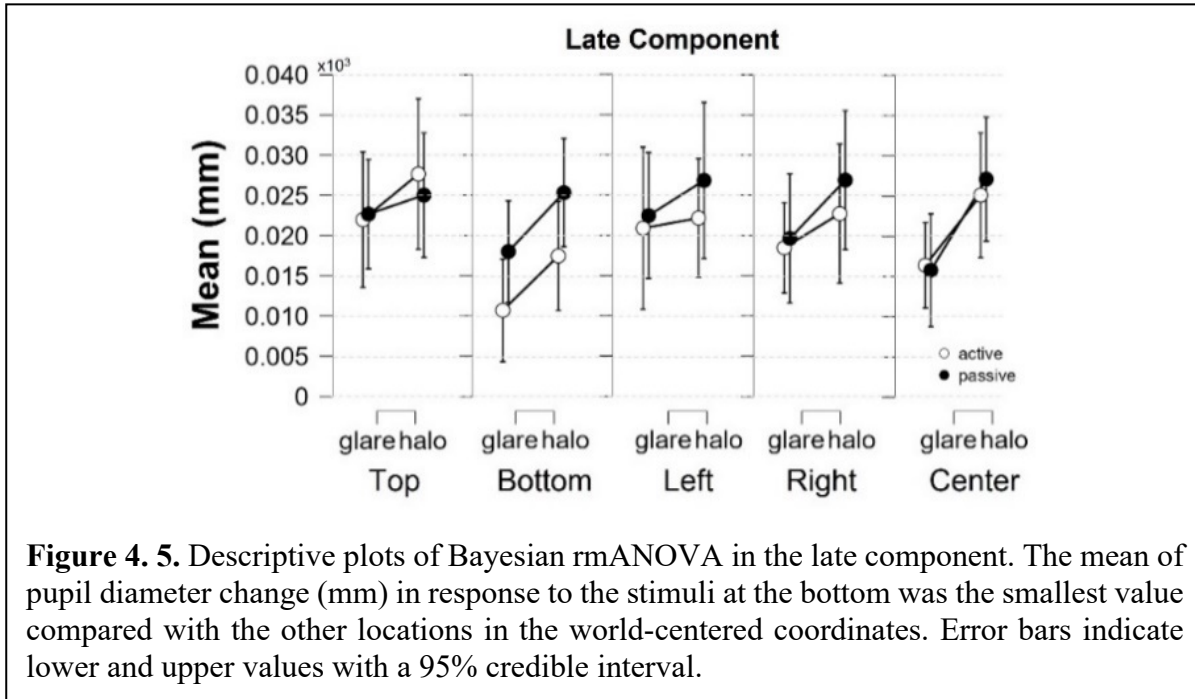


Figure 4. 5. Descriptive plots of Bayesian rmANOVA in the late component. The mean of pupil diameter change (mm) in response to the stimuli at the bottom was the smallest value compared with the other locations in the world-centered coordinates. Error bars indicate lower and upper values with a 95% credible interval.

Table 4. 5. The main effect of three-way repeated measures ANOVA in y-axis gaze data

	df	F	p	η^2_p
scene	1.000	0.157	0.697	0.009
pattern	1.000	0.480	0.498	0.027
location	2.705	2.749	0.059	0.139
scene × pattern	1.000	0.406	0.533	0.023
scene × location	2.854	2.088	0.117	0.109
pattern × location	3.087	0.842	0.480	0.047
scene × pattern × location	3.106	0.369	0.783	0.021

Table 4. 6. Model comparison using Bayesian rmANOVA in y-axis gaze data

Model Comparison						
Models	P(M)	P(M Data)	BF _M	BF ₁₀	Error %	
Null model (incl. subject and random slopes)	0.053	0.566	23.507	1.000		
pattern	0.053	0.276	6.845	0.486	8.861	
location	0.053	0.075	1.467	0.133	3.666	
pattern + location	0.053	0.032	0.593	0.056	2.686	
Scene	0.053	0.026	0.489	0.047	98.912	
Scene + location + Scene × location	0.053	0.016	0.293	0.028	93.708	
Scene + pattern + location + Scene × location	0.053	0.003	0.056	0.005	68.789	
pattern + location + pattern × location	0.053	0.002	0.037	0.004	3.033	
Scene + pattern + location	0.053	0.002	0.031	0.003	99.897	
Scene + pattern + location + Scene × pattern + Scene × location	0.053	6.867×10^{-4}	0.012	0.001	76.290	
Scene + pattern + Scene × pattern	0.053	5.223×10^{-4}	0.009	9.222×10^{-4}	70.330	
Scene + pattern + location + Scene × location + pattern × location	0.053	2.177×10^{-4}	0.004	3.845×10^{-4}	87.934	
Scene + pattern	0.053	1.094×10^{-4}	0.002	1.931×10^{-4}	54.002	

Scene + pattern + location + pattern × location	0.053	7.478×10^{-6}	1.346×10^{-4}	1.320×10^{-5}	92.223
Scene + location	0.053	5.183×10^{-6}	9.330×10^{-5}	9.152×10^{-6}	41.615
Scene + pattern + location + Scene × pattern + Scene × location + pattern × location	0.053	3.021×10^{-6}	5.438×10^{-5}	5.335×10^{-6}	71.873
Scene + pattern + location + Scene * pattern	0.053	1.987×10^{-6}	3.576×10^{-5}	3.508×10^{-6}	57.978
Scene + pattern + location + Scene × pattern + Scene × location + pattern × location + Scene × pattern × location	0.053	1.462×10^{-7}	2.632×10^{-6}	2.581×10^{-7}	97.918
Scene + pattern + location + Scene × pattern + pattern × location	0.053	1.983×10^{-8}	3.569×10^{-7}	3.501×10^{-8}	49.837

4.7 Discussion

Our previous study reported that the peripheral VFs (upper, lower, left, and right) in which the glare and halo stimuli were located influenced the subjective brightness perception of participants, as represented by the pupillary response to those stimuli [35]. The UVF generated a greater pupil dilation in response to either stimulus than did the other VFs, and reduced pupil dilation in response to the glare illusion than that in response to the halo stimulus. The results were attributed to higher-order cognitive bias formed by statistical regularity in the processing of natural scenes. However, in our previous study's results, it is possible that the differences in retinal coordinates would affect pupil size. The pupillary responses to the stimuli were influenced by pupil sensitivity, spatial resolution, and brightness perception (lower-order cognition) [9], [13], [46]. Therefore, to further investigate subjective brightness perception, not only in the peripheral VFs (our previous study's results), we conducted experiments through active and passive scenes by maintaining identical retinal coordinates and manipulating the world-centered coordinates, that is, by presenting the glare and halo as the stimuli in five different locations (top, bottom, left, right, and center) in the VR environment to investigate the anisotropy of subjective brightness perception in the world-centered coordinates. By manipulating the world-centered coordinates, we confirmed that the pupillary responses in each location differed despite the retinal coordinates being identical.

Furthermore, we divided the pupil size data into two components based on the MPCL values, that is, the early component, to evaluate the pupillary responses induced by the PLR around the area of 0.1 s before to after MPCL value, and the late component (the AUC), to access higher-order cognition (e.g., emotional arousal and subjective brightness perception) using Function 1 [35], [90], [91].

(1) The early component. Our data provide very strong evidence for the presence of stimulus patterns ($F[1,17] = 58.899$, $p < 0.001$, $\eta_p^2 = 0.776$, $BF_M = 90.205$). The significantly

constricted pupil in response to the glare compared to halo stimuli reflect the enhancement of perceived brightness [27]. In previous studies, the pupillary responses, especially during the PLR period, revealed the alteration of physical light intensity by means of lower-level visual processing [52], [87]. The PLR is elicited by visual attention, visual processing and interpretation of the visual input [52] and, possibly, higher-order cognitive involvement [40]. Hence, the low-order cognition (enhancement of brightness perception) may affect the pupillary response in the early component, as evoked by the enhancement in brightness perception. However, the early component analysis in the present study was insufficient. It had not yet fulfilled the present work's aim to elucidate whether there is an ecological advantage in the five different locations in the world-centered coordinates, which belong to high-level visual processing.

Therefore, we further investigated the pupillary response in the late component.

(2) Late component (AUC). The presence of stimulus pattern generated strong evidence ($F[1,17] = 12.437, p = 0.003, \eta_p^2 = 0.423, BF_M = 26.005$) in the effect of stimuli's physical light intensity entered the retina (low-order cognition) after the minimum peak of pupil response (MPCL). This evidence might be neither merely induced by the physical luminance of glare and halo stimuli, yet also indicated the complex visual processing.

Furthermore, our data show a significant main effect in location ($F[2.944,50.044] = 3.469, p = 0.023, \eta_p^2 = 0.169, BF_M = 0.019$). We were further investigating the post hoc comparison of location from the classical frequentist rmANOVA, and there were no significant effects in any pairs of locations. In line with the previous study by Keyers et al. (2020), we used the Bayesian factor hypothesis to overcome the absence of evidence in the post hoc comparison of location from the classical frequentist rmANOVA [95]. Considering the Bayesian factor hypothesis, the post hoc comparisons on location generated moderate evidence in the pairs of top-bottom ($t[18] = 2.586, p = 0.192, \text{Cohen's } d = 0.312, BF_{10,U} = 6.660$) and bottom-left ($t[18] = -2.927, p = 0.094, \text{Cohen's } d = -0.251, BF_{10,U} = 3.469$). Moreover, descriptive plots generated by JASP (Figure 5) exhibit the smallest mean of pupil size change in response to the stimuli at the bottom. Contrary to our hypothesis that the pupil would be most constricted in response to the stimuli at the top, we demonstrated that the response to the stimuli at the bottom obtained a higher degree of pupil constriction than the stimuli at the top location.

The highest degree of pupil constriction produced by the pupillary response to the stimuli at the bottom was linked to one of four areas in the 3D-spatial interactions model theory proposed by Previc (1998) [12]. One of those areas is the region in which a person can easily

grasp items (such as edible objects for consumption), known as the PrP region. The PrP region has a lower field bias within a 2-m radius from the observer. Objects that have already been observed are processed in the PrP region. Furthermore, the PrP region in the virtual environment, especially as the first person (FP) without an extended part of the FP (as we did in the present work), is defined by the peripheral space of the FP. It will have a large field of visual perception compared to the extended PrP region and no visual obstacle [96]. Therefore, visual processing (recognition and memorization) of objects in the PrP region requires minimal effort (an easier task for an observer's eyes). The low demand for responses to stimuli presented at the bottom in world-centered coordinates resulted in a higher degree of pupil constriction than that in response to stimuli presented at the top. In addition, statistical analysis of pupil data in the present study revealed no significant main effect of the scene in either the early or late component. This result confirmed that the head movement did not affect the pupillary response during the stimulus onset.

Considered together, the complex visual processing induced by the glare and halo stimuli and the moderate evidence from the Bayesian factor, particularly in the pair of top-bottom locations, in the late component implies that the subjective brightness perception represented by the pupillary responses to the stimuli at the top in the world-centered coordinates might be influenced by the ecological factors. For instance, first, the ecological factor evoked by the glare and halo stimuli due to the glare illusion in the present study represents the sun [25], [35]. Second, the stimuli at the top were perceived as darker than those at the bottom due to the cognitive bias related to the natural scenery where the bright blue sky is present [25]. All the evidence in our study demonstrates anisotropy of subjective brightness perception among the five locations in the world-centered coordinates. These differences in subjective brightness perception occurred even though we applied the same stimulus luminance and the same retinal coordinates across the five locations due to extraretinal information tied to the ecological factors. Moreover, the y-axis gaze angle did not seem to affect the pupil diameter, indicating identical retinal coordinates. For future studies, presenting different stimuli (e.g., the ambiguous sun and moon images) and asking the observer's perception whether the stimuli perceived as the sun or moon should be conducted to fully segregate the low-order cognition involvement on pupillary response to the stimuli.

We have two limitations in the present study. First, the eye rotation during the experiment (foreshortening with gaze angle) may have influenced the pupil size measurements in this study owing to the HMD being integrated with cameras that are used to record eye movements. We attempted to minimize this limitation during the experiment by instructing the participants to

fixate on the fixation cross. Furthermore, we rejected trials based on the fixation of the eye gaze. Second, we considered only the vertical field of world centered-coordinates due to the fact that we would elucidate whether the ecological factors (such as from the sun's existence) affect the subjective brightness perception in the world-centered coordinates. Thus, we believe that the present study offers valuable insights into the anisotropy of subjective brightness perception among the five locations (top, bottom, left, right, and central) in the world-centered coordinates, especially to understand the extraretinal information influence on subjective brightness perception in the world-centered coordinates, as revealed by using the glare illusion, manipulating the world-centered coordinates in a VR environment, and performing pupillometry. In addition, the present study provides valuable insight into the ophthalmology field that the pupillary response is not affected by head movement.

4.8 Conclusions

In the present study, we conducted the experiment by presenting the stimuli and manipulating the world-centered coordinates (top, bottom, left, right, and center) in a VR environment through active and passive scenes based on pupillary response to the glare and halo. We found anisotropy of subjective brightness perception among the five locations in the world-centered coordinates due to extraretinal information triggered by the ecological factors. In addition, we confirmed the independence of head movement in pupil diameter. In future studies, showing different stimuli (e.g., the ambiguous sun and moon images) and asking the observer's perception whether the stimuli perceived as the sun or moon should be conducted to fully segregate the low-order cognition in our results on pupillary response to the stimuli should be conducted.

Chapter 5

General Discussion

5.1 Overview of previous chapters

In this thesis, new valuable insights into the anisotropy of subjective brightness perception in VFs and world-centered coordinates revealed by pupillary response to the glare illusion have been presented. Before doing the main study, the preliminary study was conducted (Chapter 2, Paper 1). The preliminary study analyzed the pupillary responses to the ambiguous images of the sun and moon, and the results showed that the image stimuli perceived as the sun yielded larger constricted pupils than those perceived as the moon despite the image stimuli' luminance of the sun was lower than the moon. In line with the previous studies [17], [18], the finding of the preliminary study provides evidence that the perception is more predominant than the physical luminance of the stimuli image due to ecological factors such as the existence of the sun. This perception which exhibits the influence of the sun's existence (from the top) on the subjective brightness perception, will have an important account in Experiment 2's findings in this thesis project.

Furthermore, to reach the aims of this thesis, which is to critically interrogate the anisotropy of subjective brightness perception in peripheral VFs and world-centered coordinates, two approaches were presented: (1) by manipulating the retinal coordinates in the peripheral VF (Chapter 3, Paper 2), and (2) by manipulating the world-centered coordinates in a VR environment (Chapter 4, Paper 3). Both approaches were conducted by presenting the glare illusion and halo stimuli and performing the pupillometry method. Figure 5.1 shows the schematic of both approaches's results.

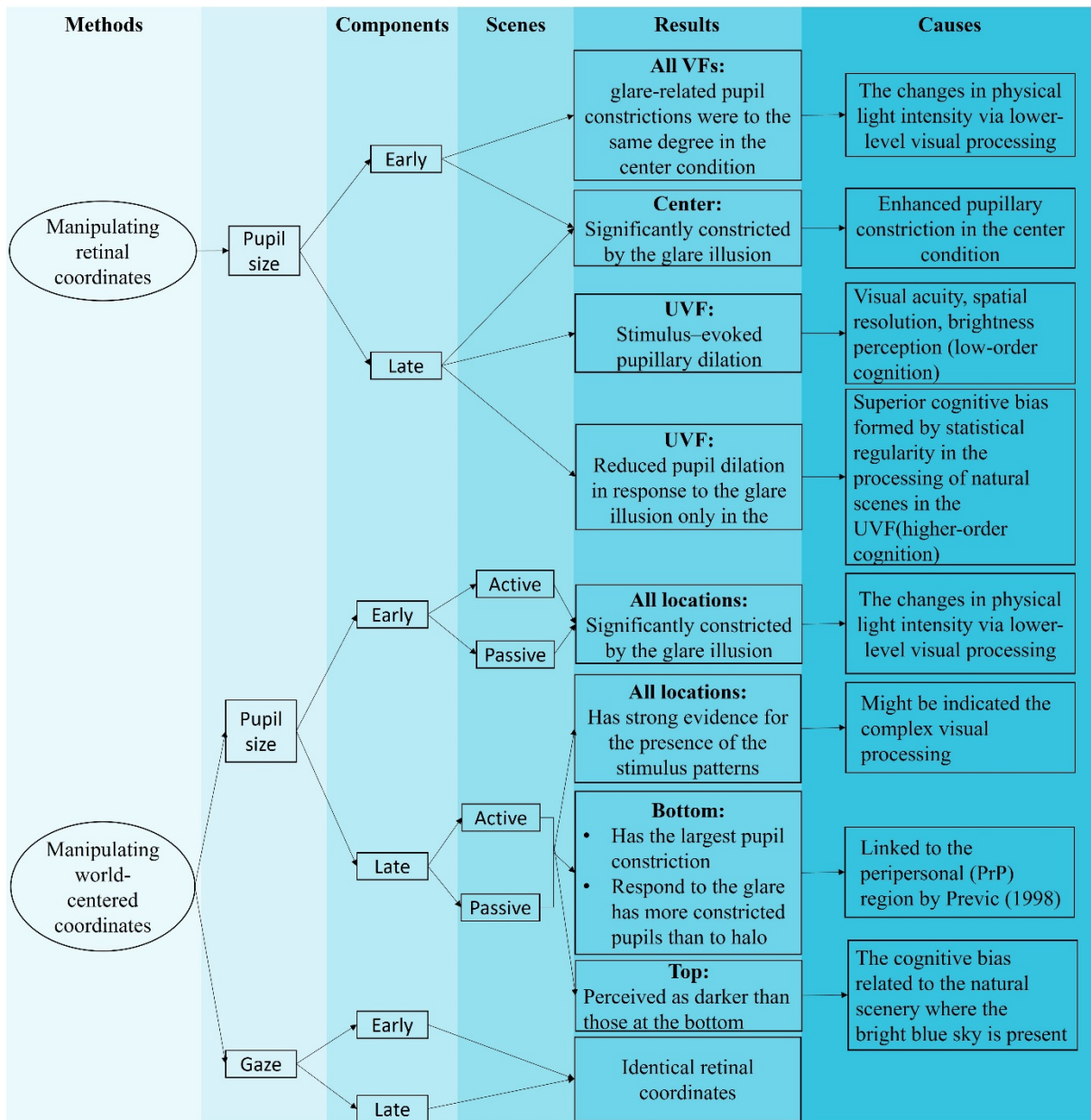


Figure 5. 1. Schematic of the main studies' results.

I. Experiment 1: by manipulating the retinal coordinates

Paper 2 (Chapter 3) elaborated on this approach to gain an understanding of anisotropy in peripheral VFs on subjective brightness perception. The results showed that the late component had a larger AUC in response to the stimuli (glare and halo) in the UVF than in the other VFs caused by the disadvantages of UVF in spatial resolution of attention [13], visual accuracy, and contrast sensitivity [9]. These UVF disadvantages (low-order cognition) evoked different visual inputs' projection in V1 and interpretation (derived from the natural world) of other VFs (retinotopic mapping) in V2. Besides, the results showed reduced pupil dilation in the UVF in response to the glare illusion compared with the other VFs. This pupillary response

was related to the self-luminosity of stimuli; thus, visual input passed to the V4 ventrally, and by combining the information from V2, the interpretation in V4 [73] might be influenced by the cognitive bias formed by statistical regularity in the processing of natural scenes in the UVF (higher-order cognition).

II. Experiment 2: by manipulating the world-centered coordinates

Paper 3 (Chapter 4) then addressed the issue of the possibility that the differences in retinal coordinates and many opponent processes in the human visual system will affect the subjective brightness perception in the VFs as the artefact of pupil size described in Paper 2. To investigate the anisotropy of subjective brightness perception in the world-centered coordinates, particularly to elucidate if there is an ecological advantage in five different positions in the world-centered coordinates based on pupillary responses to the glare illusion overtly that conveys a dazzling effect, the pupillary responses to the stimuli (glare and halo) in the VR environment have been measured and analyzed, which leads to the finding that there are the differences in subjective brightness perception in the five positions in world-centered coordinates. By manipulating the world-centered coordinates and maintaining the identical retinal coordinates, the interpretation processed in V2 would be obtained identically to the visual input. However, the findings found the subjective brightness perception differences in the world-centered coordinates. Specifically, the pupils were most constricted in response to stimuli at the bottom location. This result may be explained by the link of the bottom location to the PrP region by Previc (1998) [12]. In addition, the stimuli at the top location were perceived as darker than the bottom, which may be formed by subjective brightness perception in response to the stimuli at the top location influenced by ecological factors, e.g., the bright sky [25]. Therefore, the findings might be affected by the extraretinal information (high-order cognition). In addition, Paper 3 also demonstrates that the pupillary response is unlikely related to the head movement.

5.2 Challenges and limitations

The aims to critically interrogate the anisotropy of subjective brightness perception in peripheral VFs and rule out the low- from high-order cognition using pupillometry as an index of subjective brightness perception by manipulating the retinal and world-centered coordinates has been achieved in this study; however, the challenges and limitations of the proposed approaches were found during the study.

I. Experiment 1 (Paper 2): manipulating retinal coordinates

Previous studies in subjective brightness perception used the content of the stimuli (images or paintings of the sun and moon) and overt attention [17], [18], which is fixated on a reference object located in the middle of the stimuli [25], [97], to gain the understanding of high-order cognition relating the cognitive load triggered by the ecological factors (the sun's existence) through pupillary response. This thesis proposes the first approach (by manipulating retinal coordinates), which used the stimuli patterns (glare illusion and halo stimuli) in the peripheral VFs to stimulate the eyes in the VFs. Therefore, in Paper 2, the subjective brightness perception indexed by the pupillary changes was influenced by the combined low- (spatial resolution of attention, visual accuracy, and contrast sensitivity) and higher-order cognitions (the cognitive bias formed by statistical regularity in the processing of natural scenes) excluded the center VF that believed the higher luminance of the central white area in the central VF might influence the pupil size [10]. Another limitation in the Paper 2 is that the pupillary response to the halo in the UVF might generate dilated pupils rather than constricted pupils induced by the glare illusion. This may be due to the better contrast sensitivity in the lower, left, and right VF [79].

II. Experiment 2 (Paper 3): manipulating world-centered coordinates

Although the low- and high-order cognition have been fully segregated, there are still some problems in Paper 3. The experiments in Paper 3 required a preliminary study to record the head movement coordinates from participants beyond the main experiment. Ideally, each participant in the main experiments used a different recording of head movement coordinates which means needed 20 participants, and the recording of head movement coordinates should yield at least 90 Hz of refresh rate. However, the preliminary study in Paper 3 used only 4 participants, and due to the limitations of the recorder script developed by the author and HTC Vive Pro Eye HMD performance, the recording did not always obtain 90 frames per second (fps); thus, recording the head movement coordinates were repeated until the minimum required of fps were yielded.

Furthermore, the participants' challenge in the passive scene experiment was also found. The participants were instructed to fixate on the fixation cross located in the middle of stimuli while keeping their heads stable. As a result, the passive scene experiment was not easy because the recording of head movement coordinates was unable to move the VR environment smoothly and perfectly located the stimuli precisely in front of the participants' point of view depending on the participant of the preliminary study in Experiment 2. To overcome this limitation, the

main experiments presented a 2s fixation stage to ensure that the participants accurately fixated on the fixation cross.

5.3 Further work

Apart from addressing the above limitations, possible works to continue this thesis are discussed as follows.

Both approaches proposed in this thesis offer valuable insights into understanding the anisotropy of subjective brightness perception in peripheral VFs and world-centered coordinates. Experiment 2 demonstrated that anisotropy of subjective brightness perception is influenced by high-order cognition (extraretinal information) despite the retinal coordinates was identical. To gain further information regarding the extraretinal information that influenced the subjective brightness perception in the world-centered coordinates, testing the perception of ambiguous images of the sun and moon in a VR environment by instructing the participants to give feedback on presented ambiguous images, whether perceived as the sun or moon image and measuring the pupil diameter during the stimuli presentation. Well understanding of the extraretinal information that influenced the subjective brightness perception in the world-centered coordinates, whether caused by the cognitive load triggered by the ecological factors relating to the sun's existence, would be beneficial in informing architectural, light, and application design of a glare source (such as improving nighttime driving behavior).

Chapter 6

Conclusion

The main studies in this thesis focused on the anisotropy of subjective brightness perception in peripheral VFs and world-centered coordinates. In addition, this thesis investigated the pupillary response (as an index of subjective brightness perception) to the glare illusion and halo stimuli by manipulating the retinal coordinates (in upper, lower, left, and right VFs) and world-centered coordinates (in the top, bottom, left, right, and center positions). The summary of findings and contributions of this thesis is described as the following.

6.1 Findings

Pupil response on brightness perception. Before conducting the primary studies, the preliminary study was performed. In accordance with the previous studies [17], [18], the preliminary study of this thesis has contributed to the evidence that image perception has a more prominent role than stimuli's physical luminance by presenting ambiguous images of the sun and moon and performing pupillometry.

Subjective brightness perception in peripheral VFs. By manipulating the retinal coordinates, anisotropy of subjective brightness perception in peripheral VFs (upper, lower, left, and right VFs) occurred. Specifically, the stimulus-evoked pupillary dilation and glare-related dilated pupil reduction in the UVF due to the poor contrast sensitivity (low-order cognition) and the superior cognitive bias formed by statistical regularity in natural scene processing of the glare illusion in the UVF (higher-order cognition), respectively.

Subjective brightness perception in the world-centered coordinates. By manipulating the world-centered coordinates in a VR environment (top, bottom, left, right, and center positions), anisotropy of subjective brightness perception was found due to the influence of extraretinal information (high-order cognition). Particularly, the most dilated pupils in response to the stimuli were yielded at the top position with the head movement owing to anti-Bayesian integration in sensorimotor sensation: prior knowledge regarding stimuli at the top position may be formed by ecological factors, e.g., the sun's existence.

Correlation between the pupillary response and head movement. This thesis also confirmed the independence of head movement in pupillary response to the stimuli.

6.2 Contributions

The findings of this thesis have contributed to the following.

1. Valuable insights into understanding anisotropy in peripheral VFs and world-centered coordinates on subjective brightness perception using evidence from pupillometry and the glare illusion.
2. Would be beneficial in informing architectural, light, and application design of a glare source (such as improving nighttime driving behavior).
3. A significant contribution to the ophthalmology field owing to the findings of the independence of head movement in pupillary response to the stimuli.

References

- [1] A. Bertulis and A. Bulatov, “Distortions in length perception: Visual field anisotropy and geometrical illusions,” *Neuroscience and Behavioral Physiology*, vol. 35, no. 4, pp. 423–434, 2005, doi: 10.1007/s11055-005-0043-z.
- [2] K. Qian and H. Mitsudo, “Spatial dynamics of the eggs illusion: visual field anisotropy and peripheral vision,” *Vision Research*, vol. 177, pp. 12–19, 2020, doi: 10.1016/j.visres.2020.08.008.
- [3] Y. Sakaguchi, “Visual field anisotropy revealed by perceptual filling-in,” *Vision Research*, vol. 43, no. 19, pp. 2029–2038, 2003, doi: 10.1016/S0042-6989(03)00305-5.
- [4] Y. Wada, M. Saijo, and T. Kato, “Visual field anisotropy for perceiving shape from shading and shape from edges.,” *Interdisciplinary Information Sciences*, vol. 4, no. 2, pp. 157–164, 1998, doi: 10.4036/iis.1998.157.
- [5] S. Schwartz and K. Kirsner, “Laterality Effects in Visual Information Processing: Hemispheric Specialisation or the Orienting of Attention?,” *The Quarterly Journal of Experimental Psychology Section A*, vol. 34, no. 1, pp. 61–77, Feb. 1982, doi: 10.1080/14640748208400858.
- [6] F. H. Previc, C. Declerck, and B. de Brabander, “Why your ‘head is in the clouds’ during thinking: the relationship between cognition and upper space,” *Acta Psychologica*, vol. 118, no. 1-2 SP, pp. 7–24, 2005, doi: 10.1016/j.actpsy.2004.10.012.
- [7] S. Hong, J. Narkiewicz, and R. H. Kardon, “Comparison of pupil perimetry and visual perimetry in normal eyes: decibel sensitivity and variability,” *Investigative Ophthalmology and Visual Science*, vol. 42, no. 5, pp. 957–965, 2001.
- [8] M. Naber *et al.*, “Gaze-contingent flicker pupil perimetry detects scotomas in patients with cerebral visual impairments or glaucoma,” *Frontiers in Neurology*, vol. 9, p. 558, 2018, doi: 10.3389/fneur.2018.00558.
- [9] B. L. Portengen, C. Roelofzen, G. L. Porro, S. M. Imhof, A. Fracasso, and M. Naber, “Blind spot and visual field anisotropy detection with flicker pupil perimetry across brightness and task variations,” *Vision Research*, vol. 178, pp. 79–85, 2021, doi: 10.1016/j.visres.2020.10.005.
- [10] F. Sabeti, A. C. James, and T. Maddess, “Spatial and temporal stimulus variants for multifocal pupillography of the central visual field.,” *Vision research*, vol. 51, no. 2, pp. 303–310, Jan. 2011, doi: 10.1016/j.visres.2010.10.015.

- [11] K. Skorkovská, H. Wilhelm, H. Lüdtke, B. Wilhelm, and A. Kurtenbach, “Investigation of summation mechanisms in the pupillomotor system,” *Graefe’s Archive for Clinical and Experimental Ophthalmology*, vol. 252, no. 7, pp. 1155–1160, 2014, doi: 10.1007/s00417-014-2677-4.
- [12] F. H. Previc, “The neuropsychology of 3-D space,” *Psychological Bulletin*, vol. 124, no. 2, pp. 123–164, 1998, doi: 10.1037/0033-2909.124.2.123.
- [13] J. Intriligator and P. Cavanagh, “The spatial resolution of visual attention,” *Cognitive Psychology*, vol. 43, no. 3, pp. 171–216, 2001, doi: 10.1006/cogp.2001.0755.
- [14] F. Kingdom, “Simultaneous Contrast: The Legacies of Hering and Helmholtz,” *Perception*, vol. 26, no. 6, pp. 673–677, Jun. 1997, doi: 10.1068/p260673.
- [15] R. B. Lotto, S. M. Williams, and D. Purves, “An empirical basis for Mach bands,” *Proceedings of the National Academy of Sciences*, vol. 96, no. 9, pp. 5239–5244, Apr. 1999, doi: 10.1073/pnas.96.9.5239.
- [16] M. E. McCourt, “A spatial frequency dependent grating-induction effect,” *Vision Research*, vol. 22, no. 1, pp. 119–134, 1982, doi: [https://doi.org/10.1016/0042-6989\(82\)90173-0](https://doi.org/10.1016/0042-6989(82)90173-0).
- [17] P. Binda, M. Pereverzeva, and S. O. Murray, “Pupil constrictions to photographs of the sun,” *Journal of Vision*, vol. 13, no. 6, pp. 1–9, 2013, doi: 10.1167/13.6.8.
- [18] S. Castellotti, M. Conti, C. Feitosa-Santana, and M. M. Del Viva, “Pupillary response to representations of light in paintings,” *Journal of Vision*, vol. 20, no. 10, pp. 1–18, 2020, doi: 10.1167/jov.20.10.14.
- [19] N. Istiqomah, T. Takeshita, Y. Kinzuka, T. Minami, and S. Nakauchi, “The Effect of Ambiguous Image on Pupil Response of Sun and Moon Perception,” *International Symposium on Affective Science and Engineering*, vol. ISASE2022, pp. 1–4, 2022, doi: 10.5057/isase.2022-C000004.
- [20] J. Beatty and B. Lucero-Wagoner, “The pupillary system,” *Handbook of psychophysiology (2nd ed.)*. pp. 142–162, 2000, [Online]. Available: <http://prx.library.gatech.edu/login?url=http://search.ebscohost.com/login.aspx?direct=true&db=psych&AN=2000-03927-005&site=ehost-live>.
- [21] E. Granholm and S. R. Steinhauer, “Pupillometric measures of cognitive and emotional processes,” *International Journal of Psychophysiology*, vol. 52, no. 1, pp. 1–6, 2004, doi: 10.1016/j.ijpsycho.2003.12.001.
- [22] E. Samuels and E. Szabadi, “Functional Neuroanatomy of the Noradrenergic Locus Coeruleus: Its Roles in the Regulation of Arousal and Autonomic Function Part I:

- Principles of Functional Organisation,” *Current Neuropharmacology*, vol. 6, no. 3, pp. 235–253, 2008, doi: 10.2174/157015908785777229.
- [23] B. Laeng and U. Sulutvedt, “The Eye Pupil Adjusts to Imaginary Light,” *Psychological Science*, vol. 25, no. 1, pp. 188–197, 2014, doi: 10.1177/0956797613503556.
- [24] S. Mathôt, J. Grainger, and K. Strijkers, “Pupillary Responses to Words That Convey a Sense of Brightness or Darkness,” *Psychological Science*, vol. 28, no. 8, pp. 1116–1124, Aug. 2017, doi: 10.1177/0956797617702699.
- [25] Y. Suzuki, T. Minami, B. Laeng, and S. Nakauchi, “Colorful glares: effects of colors on brightness illusions measured with pupillometry,” *Acta Psychologica*, vol. 198, p. 102882, 2019, doi: 10.1016/j.actpsy.2019.102882.
- [26] I. K. Wardhani, C. N. Boehler, and S. Mathôt, “The influence of pupil responses on subjective brightness perception,” *Perception*, vol. 51, no. 6, pp. 370–387, May 2022, doi: 10.1177/03010066221094757.
- [27] B. Laeng and T. Endestad, “Bright illusions reduce the eye’s pupil,” *Proceedings of the National Academy of Sciences of the United States of America*, vol. 109, no. 6, pp. 2162–2167, 2012, doi: 10.1073/pnas.1118298109.
- [28] M. S. Gilzenrat, S. Nieuwenhuis, M. Jepma, and J. D. Cohen, “Pupil diameter tracks changes in control state predicted by the adaptive gain theory of locus coeruleus function,” *Cognitive, Affective and Behavioral Neuroscience*, vol. 10, pp. 252–269, 2010, doi: 10.3758/CABN.10.2.252.
- [29] Y. Kinzuka, F. Sato, T. Minami, and S. Nakauchi, “Effect of glare illusion-induced perceptual brightness on temporal perception,” *Psychophysiology*, vol. 58, no. 9, Sep. 2021, doi: 10.1111/psyp.13851.
- [30] Wikipedia contributors, “Visual system,” *Wikipedia*, 2022. https://en.wikipedia.org/wiki/Visual_system (accessed Jun. 29, 2022).
- [31] B. for ai Wiki, “Visual cortex,” 2017. https://brain-for-ai.fandom.com/wiki/Visual_cortex.
- [32] P. S. F. T. Blind, “Higher-order visual pathways and the CVI brain.” 2021, [Online]. Available: <https://www.perkins.org/higher-order-visual-pathways-and-the-cvi-brain/>.
- [33] G. Kanizsa, “Subjective contours.,” *Scientific American*, 1976, doi: 10.1038/scientificamerican0476-48.
- [34] A. Kitaoka, *Trick Eyes*. 2005.
- [35] N. Istiqomah, Y. Suzuki, Y. Kinzuka, T. Minami, and S. Nakauchi, “Anisotropy in the peripheral visual field based on pupil response to the glare illusion,” *Heliyon*, Jun.

- 2022, doi: 10.1016/j.heliyon.2022.e09772.
- [36] G. Kanizsa, *Organization in Vision: Essays on Gestalt Perception*. Praeger, 1979.
- [37] D. Corney and R. B. Lotto, “What are lightness illusions and why do we see them?,” *PLoS Computational Biology*, vol. 3, no. 9, p. 180, 2007, doi: 10.1371/journal.pcbi.0030180.
- [38] M. Naber and K. Nakayama, “Pupil responses to high-level image content,” *Journal of Vision*, vol. 13, no. 6, pp. 1–8, 2013, doi: 10.1167/13.6.7.
- [39] J. Beatty, “Task-evoked pupillary responses, processing load, and the structure of processing resources,” *Psychological Bulletin*, 1982, doi: 10.1037/0033-2909.91.2.276.
- [40] S. Mathôt, L. van der Linden, J. Grainger, and F. Vitu, “The pupillary light response reveals the focus of covert visual attention.,” *PloS one*, vol. 8, no. 10, 2013, doi: 10.1371/journal.pone.0078168.
- [41] V. Willenbockel, J. Sadr, D. Fiset, G. O. Horne, F. Gosselin, and J. W. Tanaka, “Controlling low-level image properties: The SHINE toolbox,” *Behavior Research Methods*, vol. 42, no. 3, pp. 671–684, 2010, doi: 10.3758/BRM.42.3.671.
- [42] S. Andraszewicz, B. Scheibehenne, J. Rieskamp, R. Grasman, J. Verhagen, and E.-J. Wagenmakers, “An Introduction to Bayesian Hypothesis Testing for Management Research,” *Journal of Management*, vol. 41, no. 2, pp. 521–543, Dec. 2014, doi: 10.1177/0149206314560412.
- [43] R. Arnheim and J. J. Gibson, “The perception of the visual world,” *The Journal of Aesthetics and Art Criticism*, vol. 11, no. 2, p. 172, 1952, doi: 10.2307/426044.
- [44] F. H. Previc, “Functional specialization in the lower and upper visual fields in humans: its ecological origins and neurophysiological implications,” *Behavioral and Brain Sciences*, vol. 13, no. 3, pp. 519–542, 1990, doi: 10.1017/S0140525X00080018.
- [45] L. Tan, M. Kondo, M. Sato, N. Kondo, and Y. Miyake, “Multifocal pupillary light response fields in normal subjects and patients with visual field defects,” *Vision Research*, vol. 41, no. 8, pp. 1073–1084, 2001, doi: [https://doi.org/10.1016/S0042-6989\(01\)00030-X](https://doi.org/10.1016/S0042-6989(01)00030-X).
- [46] H. Wilhelm *et al.*, “Pupil perimeter using M-sequence stimulation technique,” *Investigative Ophthalmology and Visual Science*, vol. 41, no. 5, pp. 1229–1238, 2000.
- [47] J. Zihl, P. Lissy, and E. Pöppel, “Brightness perception in the visual field - effects of retinal position and adaptation level,” *Psychological Research*, vol. 41, no. 4, pp. 297–304, 1980, doi: 10.1007/BF00308875.
- [48] M. E. McCourt, B. Blakeslee, and G. Padmanabhan, “Lighting direction and visual

- field modulate perceived intensity of illumination,” *Frontiers in Psychology*, vol. 4, no. DEC, 2013, doi: 10.3389/fpsyg.2013.00983.
- [49] G. Aston-Jones and J. D. Cohen, “An integrative theory of locus coeruleus-norepinephrine function: adaptive gain and optimal performance,” *Annual Review of Neuroscience*, vol. 28, pp. 403–450, 2005, doi: 10.1146/annurev.neuro.28.061604.135709.
- [50] O. L. Irene E. Loewenfeld, “The pupil: anatomy, physiology, and clinical applications,” *British Journal of Ophthalmology*, vol. 85, no. 1, pp. 121–121, 2001, doi: 10.1136/bjo.85.1.121e.
- [51] M. Jepma and S. Nieuwenhuis, “Pupil diameter predicts changes in the exploration-exploitation trade-off: evidence for the adaptive gain theory,” *Journal of Cognitive Neuroscience*, vol. 23, no. 7, pp. 1587–1596, 2011, doi: 10.1162/jocn.2010.21548.
- [52] S. Mathôt, “Pupillometry: psychology, physiology, and function,” *Journal of Cognition*, vol. 1, no. 1, pp. 1–23, 2018, doi: 10.5334/joc.18.
- [53] J. Rajkowski, P. Kubiak, and G. Aston-Jones, “Correlations between locus coeruleus (LC) neural activity, pupil diameter and behavior in monkey support a role of LC in attention,” *Society of Neuroscience Abstracts*, vol. 19, p. 974, 1993.
- [54] M. de Montalembert, L. Auclair, and P. Mamassian, “‘Where is the sun’ for hemi-neglect patients?,” *Brain and Cognition*, vol. 72, no. 2, pp. 264–270, 2010, doi: 10.1016/j.bandc.2009.09.011.
- [55] D. Zavagno and O. Daneyko, “When figure-ground segmentation modulates brightness: the case of phantom illumination,” *Acta psychologica*, vol. 129, no. 1, pp. 166–174, Sep. 2008, doi: 10.1016/j.actpsy.2008.05.011.
- [56] J. Sun and P. Perona, “Where is the sun?,” *Nature Neuroscience*, vol. 1, no. 3, pp. 183–184, 1998, doi: 10.1038/630.
- [57] S. He, P. Cavanagh, and J. Intriligator, “Attentional resolution and the locus of visual awareness,” *Nature*, vol. 6598, no. 383, pp. 334–7, 1996, doi: 10.1038/383334a0.
- [58] D. Zavagno, “The phantom illumination illusion,” *Perception & Psychophysics*, vol. 67, no. 2, pp. 209–218, 2005, doi: 10.3758/BF03206485.
- [59] D. H. Brainard, “The Psychophysics Toolbox,” *Spatial Vision*, vol. 10, no. 4, pp. 433–436, 1997, doi: 10.1163/156856897X00357.
- [60] M. M. Bradley, L. Miccoli, M. A. Escrig, and P. J. Lang, “The pupil as a measure of emotional arousal and autonomic activation,” *Psychophysiology*, vol. 45, no. 4, pp. 602–607, Jul. 2008, doi: 10.1111/j.1469-8986.2008.00654.x.

- [61] V. L. Kinner, L. Kuchinke, A. M. Dierolf, C. J. Merz, T. Otto, and O. T. Wolf, “What our eyes tell us about feelings: Tracking pupillary responses during emotion regulation processes.,” *Psychophysiology*, vol. 54, no. 4, pp. 508–518, Apr. 2017, doi: 10.1111/psyp.12816.
- [62] J. Love, D. Dropmann, and R. Selker, “The jamovi project (2021).” Sydney, Australia, 2021, [Online]. Available: <https://www.jamovi.org>.
- [63] SPSS Inc., “SPSS Statistics for Windows.” SPSS Inc., Chicago, 2008.
- [64] R Core Team, *R: A Language and Environment for Statistical Computing*. Vienna, Austria: URL: <https://www.r-project.org/>, 2020.
- [65] M. de Montalembert and P. Mamassian, “The vertical-horizontal illusion in hemispatial neglect,” *Neuropsychologia*, 2010, doi: 10.1016/j.neuropsychologia.2010.07.002.
- [66] J. S. Pointer and R. F. Hess, “The contrast sensitivity gradient across the human visual field: With emphasis on the low spatial frequency range,” *Vision Research*, vol. 29, no. 9, pp. 1133–1151, 1989, doi: 10.1016/0042-6989(89)90061-8.
- [67] A. Goldstein and H. Babkoff, “A comparison of upper vs. lower and right vs. left visual fields using lexical decision,” *Quarterly Journal of Experimental Psychology Section A: Human Experimental Psychology*, vol. 54, no. 4, pp. 1239–1259, 2001, doi: 10.1080/713756008.
- [68] M. Naber, G. A. Alvarez, and K. Nakayama, “Tracking the allocation of attention using human pupillary oscillations,” *Frontiers in Psychology*, 2013, doi: 10.3389/fpsyg.2013.00919.
- [69] N. Rubin, K. Nakayama, and R. Shapley, “Enhanced perception of illusory contours in the lower versus upper visual hemifields,” *Science*, vol. 271, no. 5249, pp. 651–653, 1996, doi: 10.1126/science.271.5249.651.
- [70] D. J. Felleman and D. C. Van Essen, “Distributed hierarchical processing in the primate cerebral cortex.,” *Cerebral cortex (New York, N.Y. : 1991)*, vol. 1, no. 1, pp. 1–47, 1991, doi: 10.1093/cercor/1.1.1-a.
- [71] C. O’Connell *et al.*, “Structural and functional correlates of visual field asymmetry in the human brain by diffusion kurtosis MRI and functional MRI.,” *Neuroreport*, vol. 27, no. 16, pp. 1225–1231, Nov. 2016, doi: 10.1097/WNR.0000000000000682.
- [72] M. I. Sereno *et al.*, “Borders of multiple visual areas in humans revealed by functional magnetic resonance imaging,” *Science*, vol. 268, no. 5212, pp. 889–893, 1995, doi: 10.1126/science.7754376.

- [73] U. Leonards, T. Troscianko, F. Lazeyras, and V. Ibanez, “Cortical distinction between the neural encoding of objects that appear to glow and those that do not,” *Cognitive Brain Research*, vol. 24, no. 1, pp. 173–176, 2005, doi: <https://doi.org/10.1016/j.cogbrainres.2004.12.012>.
- [74] P. Mamassian and R. Goutcher, “Prior knowledge on the illumination position,” *Cognition*, vol. 1, no. 81, pp. 1–9, 2001, doi: 10.1016/S0010-0277(01)00116-0.
- [75] V. S. Ramachandran, “Perception of shape from shading,” *Nature*, vol. 331, no. 6152, pp. 163–166, 1988, doi: 10.1038/331163a0.
- [76] A. J. Schofield, P. B. Rock, and M. A. Georgeson, “Sun and sky: Does human vision assume a mixture of point and diffuse illumination when interpreting shape-from-shading?,” *Vision Research*, vol. 51, no. 21–22, pp. 2317–2330, 2011, doi: 10.1016/j.visres.2011.09.004.
- [77] J. V Stone, I. S. Kerrigan, and J. Porrill, “Where is the light? Bayesian perceptual priors for lighting direction,” *Proceedings of the Royal Society B: Biological Sciences*, vol. 276, no. 1663, pp. 1797–1804, May 2009, doi: 10.1098/rspb.2008.1635.
- [78] Y. Lin, S. Fotios, M. Wei, Y. Liu, W. Guo, and Y. Sun, “Eye movement and pupil size constriction under discomfort glare.,” *Investigative ophthalmology & visual science*, vol. 56, no. 3, pp. 1649–1656, Jan. 2015, doi: 10.1167/iovs.14-15963.
- [79] M. M. Himmelberg, J. Winawer, and M. Carrasco, “Stimulus-dependent contrast sensitivity asymmetries around the visual field,” *Journal of Vision*, vol. 20, no. 9, pp. 1–19, 2020, doi: 10.1167/jov.20.9.18.
- [80] R. A. Andersen, L. H. Snyder, C.-S. Li, and B. Stricanne, “Coordinate transformations in the representation of spatial information,” *Current Opinion in Neurobiology*, vol. 3, no. 2, pp. 171–176, 1993, doi: [https://doi.org/10.1016/0959-4388\(93\)90206-E](https://doi.org/10.1016/0959-4388(93)90206-E).
- [81] M. Carrasco, C. P. Talgar, and E. L. Cameron, “Characterizing visual performance fields: effects of transient covert attention, spatial frequency, eccentricity, task and set size.,” *Spatial vision*, vol. 15, no. 1, pp. 61–75, 2001, doi: 10.1163/15685680152692015.
- [82] C. P. Talgar and M. Carrasco, “Vertical meridian asymmetry in spatial resolution: visual and attentional factors.,” *Psychonomic bulletin & review*, vol. 9, no. 4, pp. 714–722, Dec. 2002, doi: 10.3758/bf03196326.
- [83] E. Amenedo, P. Pazo-Alvarez, and F. Cadaveira, “Vertical asymmetries in pre-attentive detection of changes in motion direction,” *International journal of psychophysiology : official journal of the International Organization of Psychophysiology*, vol. 64, pp.

- 184–189, Jun. 2007, doi: 10.1016/j.ijpsycho.2007.02.001.
- [84] M. W. Levine and J. J. McAnany, “The relative capabilities of the upper and lower visual hemifields.,” *Vision research*, vol. 45, no. 21, pp. 2820–2830, Oct. 2005, doi: 10.1016/j.visres.2005.04.001.
- [85] C. A. Curcio and K. A. Allen, “Topography of ganglion cells in human retina,” *Journal of Comparative Neurology*, vol. 300, no. 1, pp. 5–25, Oct. 1990, doi: <https://doi.org/10.1002/cne.903000103>.
- [86] C. Tortelli, A. Pomè, M. Turi, R. Igliazzi, D. C. Burr, and P. Binda, “Contextual Information Modulates Pupil Size in Autistic Children,” *Frontiers in Neuroscience*, vol. 16, no. April, pp. 1–10, 2022, doi: 10.3389/fnins.2022.752871.
- [87] P. Mamassian and M. de Montalembert, “A simple model of the vertical-horizontal illusion,” *Vision Research*, vol. 50, no. 10, pp. 956–962, 2010, doi: 10.1016/j.visres.2010.03.005.
- [88] M. M. Chun, “Contextual cueing of visual attention,” *Trends in Cognitive Sciences*, vol. 4, no. 5, pp. 170–178, 2000, doi: 10.1016/S1364-6613(00)01476-5.
- [89] I. Jackson and S. Sirois, “Infant cognition: going full factorial with pupil dilation,” *Developmental Science*, vol. 12, no. 4, pp. 670–679, Jul. 2009, doi: <https://doi.org/10.1111/j.1467-7687.2008.00805.x>.
- [90] V. L. Kinner, L. Kuchinke, A. M. Dierolf, C. J. Merz, T. Otto, and O. T. Wolf, “What our eyes tell us about feelings: Tracking pupillary responses during emotion regulation processes,” *Psychophysiology*, vol. 54, no. 4, pp. 508–518, 2017, doi: 10.1111/psyp.12816.
- [91] M. M. Bradley, L. Miccoli, M. A. Escrig, and P. J. Lang, “The pupil as a measure of emotional arousal and autonomic activation,” *Psychophysiology*, vol. 45, no. 4, pp. 602–607, 2008, doi: 10.1111/j.1469-8986.2008.00654.x.
- [92] J. Cohen, *Statistical Power Analysis for the Behavioral Sciences Second Edition*, 2nd ed. New York, United States of America: Lawrence Erlbaum Associates, 1988.
- [93] D. Van Den Bergh, E.-J. Wagenmakers, and F. Aust, “Bayesian Repeated-Measures ANOVA: An Updated Methodology Implemented in JASP,” Jun. 2022. doi: 10.31234/osf.io/fb8zn.
- [94] Harold Jeffreys, *The Theory of Probability*, 3rd ed., vol. Third Edit. OUP Oxford, 1961.
- [95] C. Keysers, V. Gazzola, and E. J. Wagenmakers, “Using Bayes factor hypothesis testing in neuroscience to establish evidence of absence,” *Nature Neuroscience*, vol.

23, no. 7. Nature Research, pp. 788–799, Jul. 01, 2020, doi: 10.1038/s41593-020-0660-4.

- [96] J. Lee, M. Cheon, S. E. Moon, and J. S. Lee, “Peripersonal space in virtual reality: Navigating 3D space with different perspectives,” *UIST 2016 Adjunct - Proceedings of the 29th Annual Symposium on User Interface Software and Technology*, pp. 207–208, 2016, doi: 10.1145/2984751.2984772.
- [97] H. Tamura, S. Nakauchi, and K. Koida, “Robust brightness enhancement across a luminance range of the glare illusion,” *Journal of Vision*, vol. 16, no. 1, p. 10, Jan. 2016, doi: 10.1167/16.1.10.

Publication List

Journal Papers

1. Istiqomah, N., Suzuki, Y., Kinzuka, Y., Minami, T., and Nakauchi, S. Anisotropy in the peripheral visual field based on pupil response to the glare illusion. *Heliyon* **8**, e09772, 2022. doi: 10.1016/j.heliyon.2022.e09772
2. Istiqomah, N., Kinzuka, Y., Minami, T., and Nakauchi, S. Brightness perception in world-centered coordinates assessed by pupillometry. *Behav. Sci.* **13**, 60, 2023. doi: 10.3390/bs13010060.

International Conference Papers

1. Istiqomah, N., Takeshita, T., Kinzuka, Y., Minami, T., and Nakauchi, S. The effect of ambiguous image on pupil response of sun and moon perception, International Symposium on Affective Science and Engineering 2022, Japan, pp. 1-4, May 2022.